9-2012

The Development of *Dermatonotus muelleri* (Anura: Microhylidae: Gastrophryninae)

Marissa Fabrezi

Silvia Quinzio

Javier Goldberg

Rafael O. de Sá
University of Richmond, rdesa@richmond.edu

Recommended Citation

Fabrezi, Marissa, Silvia Quinzio, Javier Goldberg, and Rafael O. de Sá. "The Development of *Dermatonotus Muelleri* (Anura: Microhylidae: Gastrophryninae)." *Journal of Herpetology* 46, no. 3 (September 2012): 363-80. doi:10.1670/11-194.

Journal of Herpetology, Vol. 46, No. 3, 363–380, 2012

The Development of *Dermatonotus muelleri* (Anura: Microhylidae: Gastrophryninae)

Marissa Fabrezi,[1,2] Silvia Quinzio,[1] Javier Goldberg,[1] and Rafael O. de Sá[3]

[1]*Instituto de Bio y Geociencias-CONICET and Museo de Ciencias Naturales, Universidad Nacional de Salta, Mendoza 2, 4400 Salta, Argentina*
[3]*Department of Biology, University of Richmond, Richmond, Virginia 23173 USA*

Abstract.—**The monophyly of Microhylidae is supported by an overwhelming accumulation of synapomorphic larval features. Despite the distinctiveness of the microhylid tadpole, few studies have focused on larval development. Microhylid larval morphology is usually described and based on standard tables that imply that developmental events at equivalent stages of overall tadpole development are independent from species-specific patterns of developmental timing. Herein, we present additional developmental data based on external morphology and field data on larval growth for the gastrophrynine microhylid *Dermatonotus muelleri*. We describe internal morphological variation (e.g., skeletal and soft systems) during larval development. The results indicate that the onset of some metamorphic changes occur earlier than those implied in current anuran developmental tables. This study provides baseline information for microhylid species that will allow comparisons of ontogenetic trajectories, heterochronic patterns influencing larval body plan, and the role of larval morphology on the adult microhylid body plan.**

The understanding of anuran larval diversity has grown in the past 40 yr owing to studies of larval morphology that describe variation and provide baseline data relevant to interpreting anuran phylogenies, larval ecology, or both (e.g., Sokol, 1975; Altig and Johnston, 1989; Larson and de Sá, 1998; Haas, 2003). These studies focused on assessing variation among tadpoles from a wide spectrum of evolutionary clades independent of their specific larval developmental patterns, because such morphological descriptions of tadpoles were based on standard staging tables. Those most commonly used tables are Nieuwkoop and Faber (1956) on *Xenopus laevis* and Gosner (1960) on *Incilius valliceps* (*Bufo valliceps* Auctorum). The consequence of basing larval descriptions on standard tables is the assumption that developmental events (e.g., toe differentiation, forelimb emergence, and tail loss) are equivalent stages of tadpole development across all taxa and that these events are not subject to species-specific patterns of developmental timing. Studies assessing morphological variation of tadpole development provide detailed information for individual species (Hall and Larsen, 1998; Hall et al., 1997, 2002) or report the effects of heterochrony on larval growth, such as delayed loss of larval features and early differentiation of adult-like traits (e.g., Downie et al., 2004; Fabrezi and Quinzio, 2008; Fabrezi et al., 2009, 2010). These studies demonstrate the richness of information derived from the analyses of the entire larval development—including timing of development—to understand anuran diversity and the reciprocal influences between larval and adult body plans.

The clade Microhylidae consists of 487 described species (Frost, 2011). New World microhylids are clustered in three clades; the largest is Gastrophryninae with 52 species and includes *Dermatonotus muelleri*. Microhylids are predominantly terrestrial (i.e., fossorial to semifossorial) and mostly inhabit tropical and subtropical lowland rain forests.

The monophyly of Microhylidae is supported by adult morphology, molecular data, and a substantial accumulation of apomorphic larval features with several autoapomorphic characters (Ford and Cannatella, 1993; Haas, 2003; Frost et al., 2006). Roelants et al. (2011) suggested that among the Neobatrachia radiation, the Microhyloidea stands out by its high evolutionary rate and low levels of homoplasy with other clades and that environmental or intrinsic factors that have limited larval evolution in other anurans played a minor role on the microhyloid radiation. Despite the distinctiveness of the microhylid tadpole, representing larval morphotype II (Orton, 1953, 1957), few studies had focused on larval development. The absence of developmental data for microhylid taxa is one of the limitations in interpreting their evolutionary history.

Herein, we describe morphological variation during larval development of the gastrophrynine microhylid *Dermatonotus muelleri* and include new characters and information derived from external morphology and field data on larval growth. Descriptions of developmental morphological variation in the lateral line system, skeletal development, and other aspects of soft morphology (e.g., tongue, digestive tract, gonads, and thyroid glands) are presented. The study provides baseline information for microhylid species that will 1) allow comparisons of ontogenetic trajectories within anurans, 2) address heterochronic patterns influencing the larval body plan, and 3) interpret the role of larval morphology on the adult microhylid body plan.

Materials and Methods

Larval *Dermatonotus muelleri* (Boettger, 1885) were collected between November and April 2000–2007 in ephemeral ponds along Ruta Nacional 81 (23°10′S, 63°39′W to 23°14′S, 63°39′W) in Departamento San Martín, Provincia de Salta, Argentina. Specimens were fixed in 10% formalin in the field. Lots of specimens are deposited in the Herpetological Collection of the Museo de Ciencias Naturales (MCN), Universidad Nacional de Salta, Argentina, with the following collection data: MCN 1162 (25 November 2000), MCN 1163 (17 January 2000), MCN 672 (2 January 2001), MCN 1102 (11 November 2002), MCN 1016 (4 March 2004), MCN 946 (11 December 2004), MCN 960 (19 December 2004), MCN 1094 (29 December 2004), MCN 1080 (12 March 2005), MCN 1180 (13 April 2005), MCN 1066 (18 December 2005), MCN 1009 (28 December 2005), MCN 1357 (28 November 2007), 1358 (12 December 2007), MCN 1340 (27 December 2007), and MCN 1332 (5 January 2008), and six adult specimens that are deposited with lot MCN 997.

We selected 70 specimens from lots MCN 1332, 1357, 1358, and 1340 to include individuals in a larval series ranging from hind limb bud stages up to absence of the tail stage. Specimens of these lots were collected from the same pond and had started

[2]Corresponding Author. E-mail: mfabrezi@aol.com
DOI: 10.1670/11-194

TABLE 1. Comparisons of key features between anuran larval stages by Gosner (1960) and larval stages of *Dermatonotus muelleri* (this study).

Gosner larval stages	*D. muelleri* stages
26–30: Limb bud length from one-half diameter to twice diameter. Complete mouthparts.	26–30: Limb bud length from one-half diameter to twice diameter. Complete mouth, upper lip with well differentiated alae.
31–34: Paddle-like foot. Interdigital indentations.	31–34: The pointed foot is clearly defined by the elongation of primary axis. Interdigital indentations.
35–37: Stabilized pigmentary patterns. Toe development.	35–37: Maximum larval size. Toe development progresses as outgrowths in the proximo-distal direction. Interdigital membranes are absent.
38–39: Metatarsal and subarticular tubercles.	38–39: Metatarsal and subarticular tubercles. Dark pigmentation. External nostril perforated.
40: Loss of vent tube.	40: Loss of vent tube. Anterior displacement of spiracle. Appearance of skin lateral patches of forelimbs. Alae of upper lip with ventrolateral dark projections.
41: Maximum larval size. Breakdown of larval mouthparts.	41: Snout uplifted and nostrils protruded. Forelimbs protruding.
42: Forelimbs emergence. Absence of larval mouthparts. Angle of mouth anterior to the nostril.	42: Forelimbs emergence. Alae of upper lip reduce up to disappearance. Angle of mouth anterior to the nostril. Spiracle reduced to a medial and an oval opening on the ventral wall.
43: Angle of mouth between nostril and the midpoint of eye. Presence of tongue. Regression of dorsal and ventral fins.	43: Upper lip conserving dark vestiges of the alae. Angle of mouth between nostril and the anterior border of the eye. Dorsal fin becomes lower. Spiracle opening is positioned behind forelimbs.
44: Angle of mouth between the midpoint and the posterior margin of eye. Caudal musculature greatly reduced.	44: Angle of mouth reaches the anterior border of eye. Spiracle scarf is still present. Caudal fins and tail musculature well differentiated. Eyelids.
45: Angle of mouth at the posterior margin of eye. Tail reduced to stub.	45: Angle of mouth reaches the mid-level of the eye. Strong shortness of the tail, musculature and fins are indistinct. Vestige of spiracle has disappeared. Differentiation of the nictitant membrane.
46: Tail completely resorbed. Angle of mouth may be positioned caudal the posterior margin of eye.	46: Tail reduced to a dehiscent stub or absent. Angle of mouth between the mid-level and the posterior margin of eye.

to develop at the end of November 2007. Initial staging of larvae followed that of Gosner (1960). Table 1 provides additional species-specific features of *D. muelleri* to complement Gosner's larval stages. Parameters of larval growth were inferred from variation in body length (i.e., distance between snout and posterior end of the body) and total length (i.e., distance between snout and tip of the tail in lateral view). Measurements were made with dial calipers (0.02 mm) and are given in millimeters.

Larval development includes description of morphological changes in external and internal morphology. Morphological features of the lateral line system were recorded with a stereomicroscope; line drawings were made with the aid of a camera lucida and images were recorded with a digital camera. Topography of neuromasts follows that of Lannoo (1987), with modification of the terminology for the orbital lines. Descriptions of neuromasts and photographs were made with a scanning electron microscopy (SEM) at the LASEM (Laboratorio de Microscopía Electrónica de Barrido, ANPCyT/UNSa/CONICET), Salta, Argentina. Pieces of the skin from the dorsal, lateral, and ventral body wall of tadpoles at different developmental stages were taken for SEM examination and processed following the technique of Bozzola and Russell (1999).

We used cleared and double-stained (i.e., for bone and cartilage) specimens to examine skeletal variation. Specimens were prepared using the technique of Wassersug (1976). Preserved specimens were dissected to analyze anatomical changes in the gonads, digestive tract, thyroid glands, and the tongue and associated muscles. Stages of gonadal differentiation followed Ogielska and Kotusz (2004). Descriptions, illustrations, and photographs were made with the aid of a Nikon SMZ1000 stereo dissection microscope equipped with an 8.1-megapixel digital camera.

We examined transverse sections of tadpoles at stages 35 and 43 to analyze histological changes in the thyroid glands and operculum. Formalin-preserved tadpoles were dehydrated, embedded in paraffin, sectioned at 6 μm, and stained with hematoxylin and eosin following the protocol of Martoja and Martoja-Pierson (1970). Observations and photographs were made with Leica DM EP compound microscope equipped with digital camera.

Larval and adult specimens of *Elachistocleis bicolor* (MCN 797, MCN 691, MCN 945, MCN 797, MCN 996, MCN 1010) and adult *Phrynomantis bifasciatus* (MCN 830), *Gastrophryne carolinensis* (FML 3365), and *Scinax acuminatus* (MCN 800) were used for morphological comparisons. Museum abbreviations are as follows: FML, Instituto de Herpetología, Fundación Miguel Lillo, Tucumán, Argentina; and MCN, Museo de Ciencias Naturales, Universidad Nacional de Salta, Argentina.

Anatomical terminology is based on the amphibian anatomical ontology (www.amphibanat.org).

RESULTS

Larval Stages Based on External Morphology.—The development of *D. muelleri* is summarized and compared with standard Gosner's stages (Table 1; Fig. 1).

Stages 26–37: These stages are based on hind-limb development and toe differentiation. Morphology of the developing limbs resembles that of *Elachistocleis bicolor* (Goldberg and Fabrezi, 2008). Throughout these stages, the color in life and in preservative of tadpoles is uniform, ranging from clear greenish to dark brownish in different individuals; the skin is opaque and only the tail fins are transparent. During this period, the upper labium of the terminal mouth grows and reaches the fully developed tadpole morphology, i.e., well-differentiated and quadrangular alae separated by a rounded notch; it completely

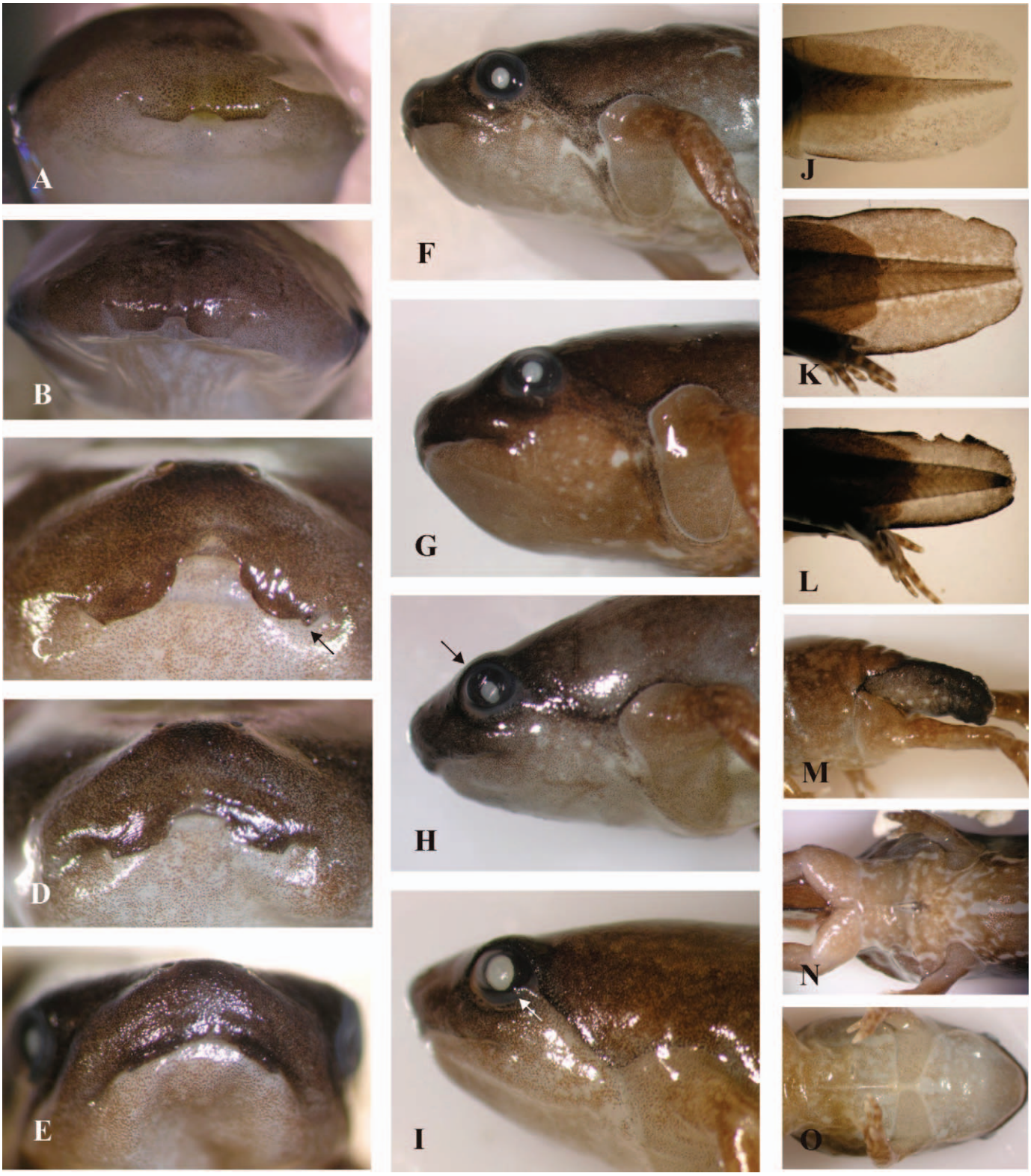

FIG. 1. Changes in external morphology during larval development and metamorphosis in *Dermatonotus muelleri*. (A–I) Mouth transformations. (A) Stage 28, frontal view. The upper labium is divided by a medial notch into two quadrangular flaps overlapping the lower labium. (B) Stage 35, frontal view. (C) Stage 39, frontal view. Each flap presents rounded border and a fang-like latero-external projection. At this stage, the nostrils are perforated. (D) Stage 42, frontal view. (E–F) Stage 43, frontal and lateral views respectively. The larval mouth becomes different. Upper labium is straight without the medial notch and flaps. Lower labium is now visible. Angle of the mouth is placed between the nostril and the eye. (G) Stage 44, lateral view. Angle of the mouth reaches the anterior margin of the eye. (H) Stage 45, lateral view. Angle of the mouth is positioned at the midpoint of the eye. Upper eyelid has appeared. (I) Stage 46, lateral view. Angle of the mouth is located between the midpoint and the posterior margin of eye. The nictitacting membrane is evident. (J–M) Tail changes. (J) Stage 28. Dorsal and ventral fins are symmetrical and tall. (K) Stage 42. Pigmentation is evident in fins. (L) Stage 44. Fins become lower. (M) Stage 45. Tail is an atrophied stub. (N) Stage 43, ventral view. There is a medial scarf representing the vestigial spiracle. (O) Stage 44, ventral view. The body wall presents different patterns of pigmentation. Scale bar = 2 mm.

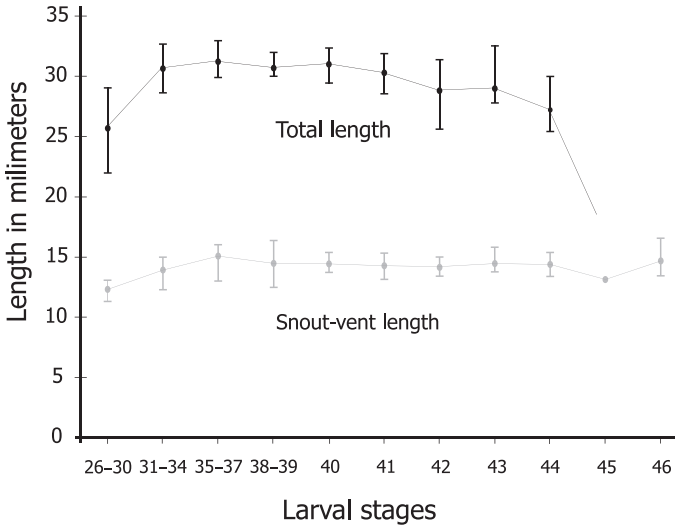

FIG. 2. Mean, maximum, and minimum values of total lengths and SVLs during larval development of *Dermatonotus muelleri* ($N = 64$).

overlaps the lower jaw (Fig. 1A, B). The spiracle is posteromedial in position and opens slightly anterior and ventral to the vent tube; the vent tube is short, funnel-shaped, and attached to the ventral fin. External nostrils, eyelids, and nictitating membranes are absent. The tail conserves its shape during the period (Fig. 1J).

Stages 38 and 39: The metatarsal tubercle and subarticular tubercles on the toes develop in this period. The external nostrils open. The alae of the upper labium are oriented obliquely and have "fang-like" ventrolateral projections (Fig. 1C). The vent tube is anteriorly adjacent to the origin of the ventral fin. Dorsally, the tadpole is uniformly dark, whereas the abdomen is patterned with discontinuous, longitudinal, and dark stripes on a whitish background. The hind limbs are dark.

Stage 40: The vent tube is absent and the cloacal opening is developed. The reduced spiracle is located farther anterior on the ventral wall of the body than before. Anteriorly on the ventrolateral sides of the body, rounded and uniformly pigmented patches of skin mark the position where the forelimbs will emerge.

Stage 41: The tadpole's snout begins to resemble that of the adult. It is slightly uplifted and acquires an overall pointed appearance; external nostrils are prominent and the mouth opening is ventral. In dorsal view, the forelimbs begin to protrude through the lateral body wall.

Stage 42: The forelimbs have emerged. The forelimb skin has a distinct line marking the union of the forelimb with the skin of the body wall. The upper labium of the larva has begun to disappear in the region of the lateral alae, but the "fang-like" projections are still visible (Fig. 1D); the mouth is now transversely oriented. The spiracular opening remains. The dorsal fin decreases in height, but the tail length does not change (Fig. 1K).

Stage 43: The mouth opening widens and the angle of the jaw lies between the nostril and the eye. The alae of the upper labium have almost disappeared (Fig. 1E, F), and the spiracle lies farther anterior, with the spiracular opening being posterior to the forelimbs (Fig. 1N).

Stage 44: The angles of the jaws are located at the level of the anterior border of the eyes at stage 44 (Fig. 1G). The

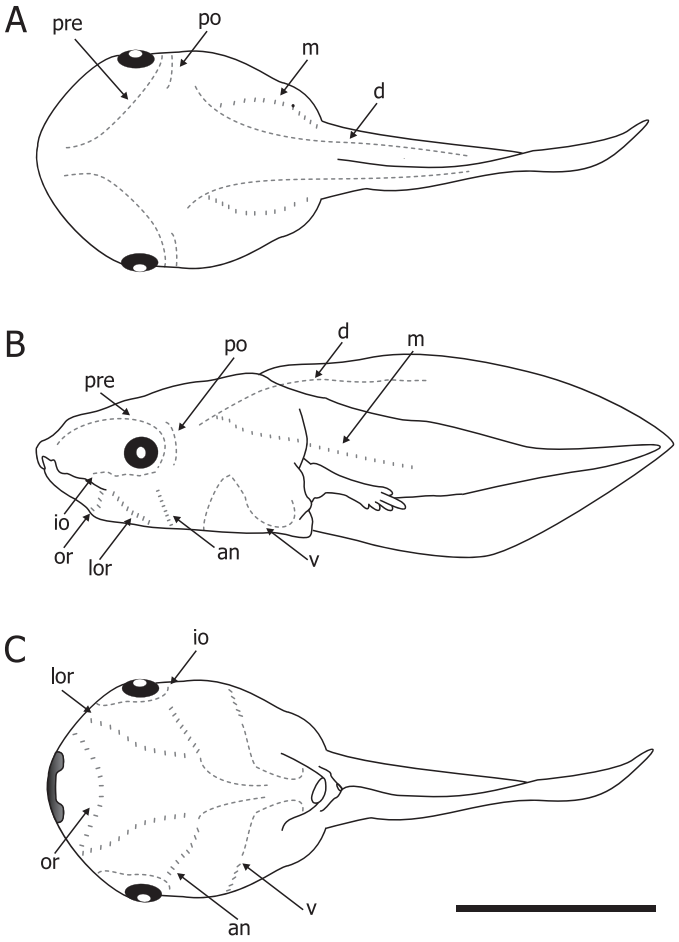

FIG. 3. Lateral line system of *Dermatonotus muelleri* at stage 36. (A) Dorsal view. (B) Lateral view. (C) Ventral view. The lateral lines are sketched with the groups of neuromasts (dashes) as observed in preserved specimens. The individual groups of neuromasts are not drawn to scale. Abbreviations: an, angular line; d, dorsal line; io, infraorbital line; lor, longitudinal oral line; m, medial line; or, oral line; po, postorbital line; pre, preorbital line; and v, ventral line. Scale bar = 10 mm.

spiracular opening is a longitudinal slit. The caudal fins are lower (Fig. 1L), and the eyelids are incipient (Fig. 1G).

Stage 45: The angles of the jaws lie at the midlevel of the eyes (Fig. 1H), and the spiracle is absent. The tail is substantially shorter, and the fins and musculature are atrophied (Fig. 1M). The nictitating membrane begins to differentiate (Fig. 1H).

Stage 46: The disappearance of larval structures at stage 46 marks the end of the metamorphosis. The angles of the jaws extend slightly posterior to the midlevel of the eyes (Fig. 1I), and the atrophied tail stub is short or absent. The ventral surface of the body has well-defined, colored areas, i.e., gular, pectoral, and ventral areas (Fig. 1O). The eyelids and nictitating membrane are not fully developed (Fig. 1I).

Size and Timing of Larval Development.—Larval somatic growth increases until stage 37 when the tail length is about equal to snout–vent length (SVL; Fig. 2) and the SVL is at its maximum, corresponding to the size of the metamorphosed individuals (≈14 mm). During metamorphosis, total length decreases owing to tail resorption that occurs abruptly in stage 45. The postmetamorphic size is approximately 3 times the size at metamorphosis, with adults being 40–50 mm. Development,

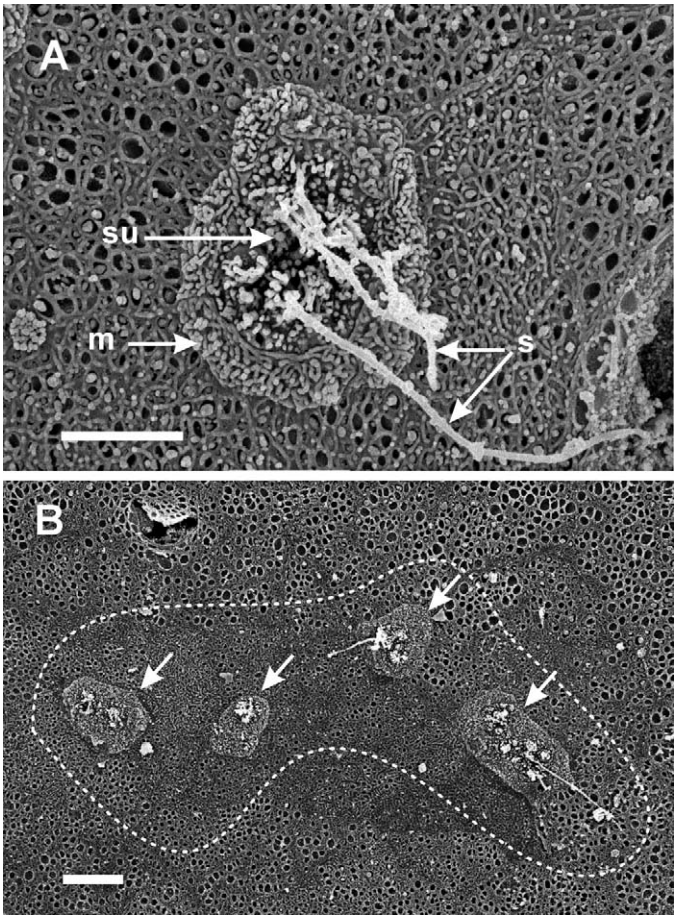

FIG. 4. SEMs of neuromasts of *Dermatonotus muelleri* larvae at stage 36. (A) Individual neuromast of the dorsal lateral line. Scale bar = 5 μm. (B) Group of neuromasts (white arrows) of the dorsal lateral line, note the irregular distribution of the organs. Scale bar = 10 μm. Abbreviations: m, mantle cells; s, sensory cells; and su, supporting cells.

from fertilization to the end of metamorphosis, occurs in 25–30 days.

Anuran larval development is characterized by three functional developmental periods: 1) differentiation, development, and disappearance of unique larval features; 2) remodeling of larval into adult structures during metamorphosis; and 3) differentiation and development of adult structures.

Disappearance of Larval Traits.—Among the larval structures that disappear are the oral structures, vent tube, spiracle, and tail; these structures have been described in other studies (e.g., Gosner, 1960; Duellman and Trueb, 1986; Fabrezi, 2011). Herein, we focus on the lateral line system.

Tadpoles throughout stages 26–39 have a lateral line system consisting of nine pairs of lateral lines—three pairs of orbital lines, three pairs of mandibular lines, and three pairs of trunk lines (Fig. 3). The orbital lines are the preorbital (pre), infraorbital (io), and postorbital (po). Preorbital and infraorbital lines are continuous with each other behind the eye and extend anteriorly dorsal and ventral to the eye respectively (Fig. 3B). The postorbital line lies posterior to the confluence of the preorbital and infraorbital lines and is anteriorly concave. Mandibular lines comprise the oral (or), longitudinal oral (lor), and angular (an) lines that are visible on lateral and ventral views (Fig. 3B, C). The oral line runs between the angle of the mouth forming a ventral semicircle. The longitudinal oral lines extend from the angle of the mouth, posterior to the oral line, and run ventrally and posteriorly. The angular lines originate below the posterior margins of the eyes and descend between the longitudinal oral lines and the ventral lines. The angular lines converge ventrally without contacting with each other and terminate anterior to the ventral line and the spiracle (Fig. 3C). The trunk lines are the dorsal (d), medial (m), and ventral (v). The dorsal line originates behind the postorbital line (internally at the level of the posterior margin of the otic capsule) and extends upward along the trunk and the anterior third of the dorsal fin (Fig. 3A, B). The medial line diverges from the dorsal line and runs along the trunk and the hypaxial musculature of the tail for about half the length of the tail. Laterally, the ventral line resembles a horizontal S. The anterior arm of the S descends and runs posteriorly to converge at midlength of the spiracle with its contralateral member (Fig. 3C).

The lateral lines resemble dashed lines under stereomicroscopy. Each dash consists of two to six neuromast organs. SEM images reveal that each neuromast organ is circular, with its perimeter defined by an outer layer of mantle cells surrounding a central area that consists of the sensory cells surrounded by microvilli of the supporting cells (Fig. 4A). The neuromasts are as much as 20 μm across and are located in shallow depressions of the epidermis with a variable number of sensory cells (three to six, Fig. 4B).

The orientation of the dashes in a lateral line varies. For example, in the oral, longitudinal oral, and medial lines, the main axis of the dashes are perpendicular to the orientation of the line, whereas in other lines, the axes are parallel to the orientation of the line. There is also variation in the orientation of the dashes along some lines; for example, along the angular and ventral lines, the dashes gradually shift from a perpendicular to parallel orientation.

The lateral line system is considerably reduced by stage 40. The preorbital, infraorbital, oral, and longitudinal oral lines are shorter, and the neuromasts of the dorsal and medial lines disappear along the trunk. The angular and ventral lines are anteriorly displaced concomitant with the displacement of the spiracle. The ventral line is disrupted by the appearance of lateral patches of skin marking the development of the forelimbs. During stage 42, the neuromasts of the preorbital line are restricted to the area between the nostrils. In addition, the postorbital line is shortened and the infraorbital, oral, and longitudinal oral lines have completely disappeared; the neuromasts of the angular and ventral lines are smaller. By stage 43, the preorbital, postorbital, angular, and ventral lines are absent, but the neuromasts of the medial line along the caudal musculature are still present. By stage 45, all neuromasts have disappeared.

Remodeling of Larval Traits during Metamorphosis.—Several tissues, organs, and organ systems that differentiate in early larval stages subsequently are remodelled to become adult structures. Herein, we describe the sequence of developmental events and the timing of changes in the digestive tract, chondrocranium, and hyobrachial skeleton.

Tadpoles in stages 26–39 characteristically have a long intestine that is nearly uniform in diameter with a thin and almost transparent wall. The foregut is located on the right side of the abdominal cavity and forms a U-loop around an elongated pancreas. Anteriorly the hindgut turns and forms a double spiral placed on the left side of the abdominal cavity. In contrast, the posterior hindgut is coiled into a double spiral that is medial in position, with the most inner segment opening into

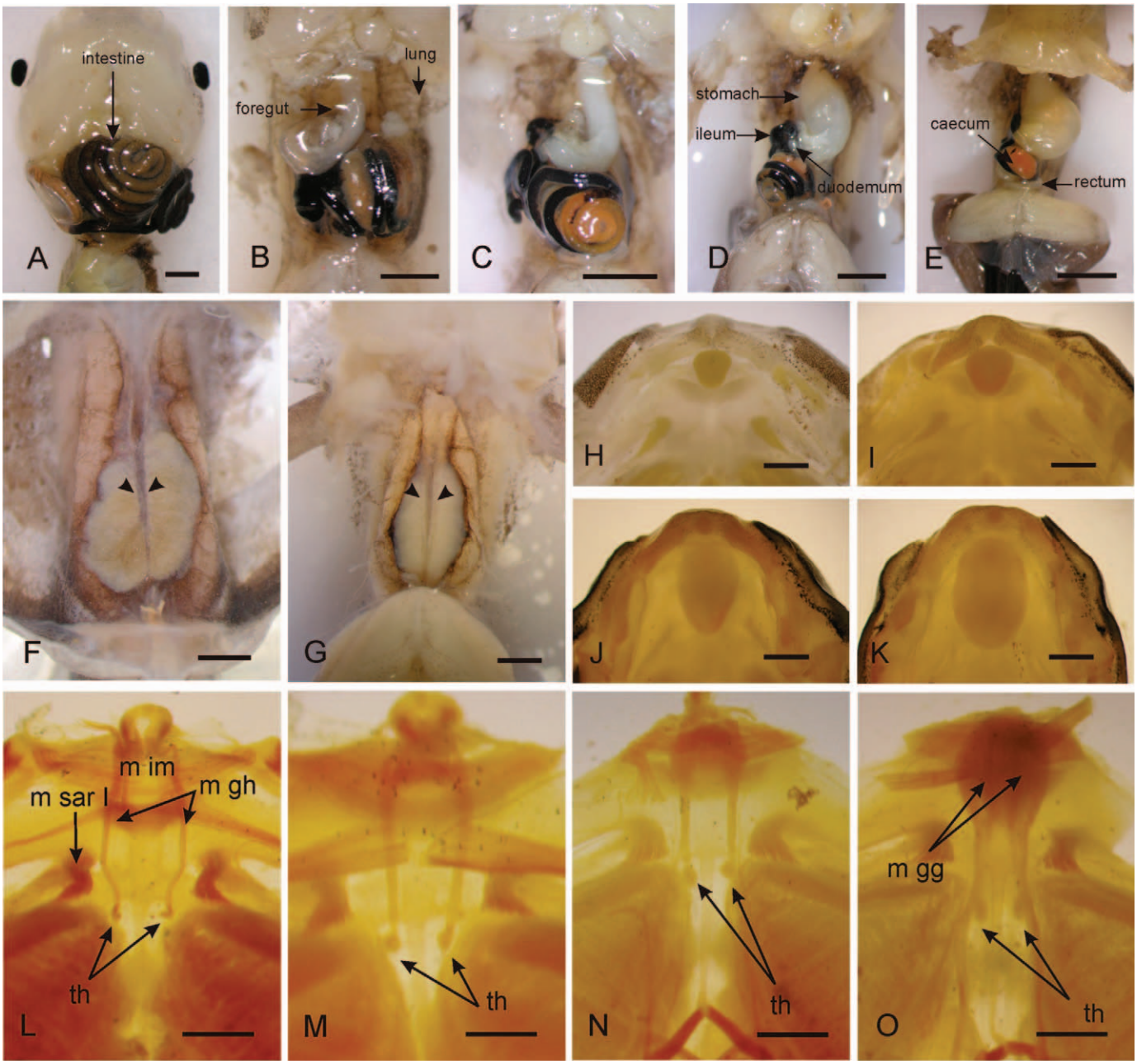

FIG. 5. Morphological changes in soft organs during development of *Dermatonotus muelleri*. (A–D) Gut transformations, scale bar = 2 mm. (A) The long spiralled larval intestine occupies the entire abdominal cavity at stage 31. (B) The intestine decreases in diameter and the anterior portion enlarges, becomes thicker and distinct from the posterior gut at stage 40. (C) Differentiation of stomach, duodenum and ileum advances at stage 42. (D) The stomach is well differentiated and there is a constriction separating stomach from duodenum at stage 44. (E) Posteriorly, the hindgut is differentiated in the rectum and a dilated caecum before ending into the cloaca. Undifferentiated gonads at stages 32 (F) and 44 (D). Arrows points the cord precursors. Scale bar = 1 mm. (H–K) Tongue development. Scale bar = 1 mm. Stages 37, 40, 43, and 45. The tongue anlage is a cordiform mass in the buccal floor immediately posterior the infrarostrals and grows posteriorly to cover the entire buccal floor. At the end of larval development, the tongue is oval-shaped. (L–O) Changes in the thyroid glands during development. Scale bar = 1 mm. (L) The glands comprise a pair of distinct masses ventral and lateral to the basibranchial during stage 28, they enlarge during further development. The thin muscle geniohyoideus with diffuse origin in the proximity of the thyroid gland is one of the autoapomorphic characters of microhylid tadpoles (Haas, 2003). (M) Stage 33. (N) Stage 36. (O) Stage 43. Abbreviations: m gh, muscle geniohyoideus; m gg, muscle genioglossus; m ih, muscle interhyoideus; m im, muscle intermandibularis; m sar I, muscle subarcualis rectus I; and th, thyroid gland.

the cloaca (Fig. 5A). The pancreas and an incipient liver lie to the right and overlap the foregut. Lungs are inflated and lie dorsolateral to the liver and intestine.

At stage 40, thin, transparent layers of tissue cover the abdominal cavity where a few longitudinal muscular fibers insinuate the development of the rectus abdominis muscle. The liver consists of three large lobes occupying the anterior portion of the abdominal cavity, and a large gall bladder lies among the lobes on the caudal portion of the liver. The foregut is dilated; it has lost its U shape and become straight, thicker, and distinct from the hindgut that has decreased in diameter. The anterior intestinal coils lack an organized pattern of turns; the posterior hindgut is dilated and located in the midline (Fig. 5B).

Between stages 41 and 43, four pairs of clustered muscle fibers differentiate in the ventral wall of the body to initiate the adult arrangement of the adult rectus abdominis muscle. Overall, the walls of the foregut thicken and the hindgut shortens.

At stage 44, the foregut has a differentiated and expanded stomach morphologically defined by anterior and posterior sphincters that separate it from the oesophagus and the intestines, respectively. The anterior hindgut is curved but does not spiral as seen in the posterior hindgut (Fig. 5C). By stage 45, the distal portion of the hindgut is larger in diameter and forms the rectum, and the rectum has a dilated caecum (Fig. 5D).

The chondrocranium and hyobrachial skeleton of *D. muelleri* tadpoles in stages 31–37 (Fig. 6A) were described by Lavilla (1992) and Vera Candioti (2007). Herein, we describe developmental changes in the chondrocranium starting at stage 38.

Similar to previous stages, the neurocranium is broad; its length is ≈78% of its greatest width at level of the otic region. Cartilaginous structures roofing the cavum cranii are absent, and it is delimited by the tectum synoticum (posterior), the tectum nasi (anterior), and the orbital cartilages (lateral). The ethmoidal region and the olfactory tracts are short. The otic capsules are elongated (≈25% longer than wide) and oriented with their long axis slightly divergent from the sagittal plane. The septum nasi is broad and positioned medially and transversely to the ethmoidal plate (Fig. 6A). The ethmoidal plate extends anteriorly beyond the septum nasi to the level of the processes quadrato-ethmoidalis, diverging into short and distally expanded cornua trabeculae. At the same time, the tectum nasi is developed and it is posteriorly continuous with the laminae orbitonasales. The palatoquadrate has a short and robust pars articularis quadrati, a broad commissura quadratocranialis anterior, a broad and low processus muscularis (oriented slightly outward), and a relatively narrow and straight arcus subocularis that terminates in a stout and outwardly projecting cartilaginous bar, the pars posterior. The palatoquadrate attaches to the braincase by three cartilaginous bridges. (1) The broad commissura quadratocranialis anterior (diverging anteriorly in approximately a 45° angle with the main chondrocranial axis) joins the anterior portion of the palatoquadrate to the trabecular plate. (2) The processus ascendens diverges toward the braincase from the arcus subocularis at the level of the pars posterior and links the palatoquadrate with the orbital cartilage. (3) The larval processus oticus is ventrally continuous with the pars posterior and dorsally with the processus anterolateralis of the crista parotica. On the ventral surface of the pars posterior there is a narrow posterior process extending backward. Behind the larval processus oticus and extending from the otic capsule, a broad and thin cartilage extends ventrally and is continuous with the posterior edge of the pars posterior; this lamina is extensively perforated. The suprarostral is a single laminar cartilage with a medial concavity, which provides the skeletal support for the upper lip alae. The distal ends of the cornua trabeculae are expanded and straight and each half of the suprarostral is extensively fused with the anterior margin of each cornu. The lower jaw consists of a single infrarostral that is a slender element forming an inverted U-shaped structure, with lateral cartilaginous expansions representing the Meckelian diverticula (Fig. 6F, G) and a pair of lateral Meckel's cartilages. Meckel's cartilages are transverse bars with acuminate and pointed medial tips that are contiguous to the infrarostral; the outer ends are broad, robust, and articulate with the pars articularis of the palatoquadrate.

Changes in the ethmoidal region begin at stage 39 (Fig. 6B). The septum nasi is now slender. The paired anterior nasal walls grow laterally to the anterior end of the septum nasi. At this stage, the anterior nasal walls remain independent from the trabecular plate. Furthermore, the posterior nasal wall lifts up from the commissura quadratocranialis anterior.

By stage 40, the septum nasi has grown anteriorly reaching the divergence of the trabecular horns. The alary cartilages are visible as small, slender, elements located in front of the septum nasi on the trabecular plate. The alary cartilage is continuous with the anteriorly placed inferior prenasal cartilage and laterally with the developing laminae superior and inferior crista intermedia. The septum nasi projects forward as a short median prenasal process. The developing oblique cartilages are L-shaped, with the longer and transversely positioned arm being continuous with the septum nasi. The planum triangulare has been differentiated.

At stage 41, the erosion of the cornua trabeculae has begun and the cartilages of the nasal capsule form a complex structure. The incipient crista subnasalis develops ventral to the alary cartilages. The anterior and posterior nasal walls and the planum triangularis rise up bordering the commissura quadratocranialis anterior. The processus muscularis of palatoquadrate and the posterior cartilaginous connections between the palatoquadrate and the braincase have begun to erode. The suprarostral is still present, but resorption has started and progresses from medial to lateral direction.

By stage 42 (Fig. 6C), the cornua trabeculae are absent. Erosion of the suprarostral has advanced resulting in two lateral free pieces. The snout of the tadpole now is truncate in profile and composed of the frontal alary cartilages and the processus prenasalis. The oblique cartilages, as well as the laminae superior and inferior crista intermedia, are vertical in position. Ventrally, the crista subnasalis is massive and its posterior process is well defined. The nasal walls have grown and the planum triangularis has a processus maxillary anterior. The tectum nasi has expanded anteriorly and laterally covering the septum nasi along its length. The commissura quadratocranialis anterior is slender. Meckel's cartilages and infrarostral have started to undergo morphological reshaping and fusion. The infrarostral forms a transverse bar with a distinct cartilaginous medial union. Lateral and ventral to the "mandibular symphysis" the pair of Meckelian diverticula became massive (Fig. 6H). Meckel's cartilages are longer and oriented obliquely.

The medial and anterior cartilages of the nasal capsule have grown into a well-developed complex by stage 43. The commissura quadratocranialis anterior seems to be fused to the planum triangulare, forming a new anterior attachment of the palatoquadrate to the neurocranium. Erosion of the arcus subocularis has advanced anteriorly. The processus articularis is slender and rounded. The lower jaw lengthens concomitantly with the processus pterygoideus that represents the posterior growth of most lateral portion of the commissura quadratocranialis anterior.

By stage 44 (Fig. 6D), the cartilaginous snout nearly has its adult form. The processus pterygoideus is curved, short, and continuous with the pars articularis of palatoquadrate that is now expanded, rectangular, and well differentiated. The cartilaginous pars articularis is perpendicularly oriented to the processus pterygoideus, and its anteroventral tip is modified to articulate with the Meckel's cartilage. Lengthening of the Meckel's cartilage continues throughout this stage.

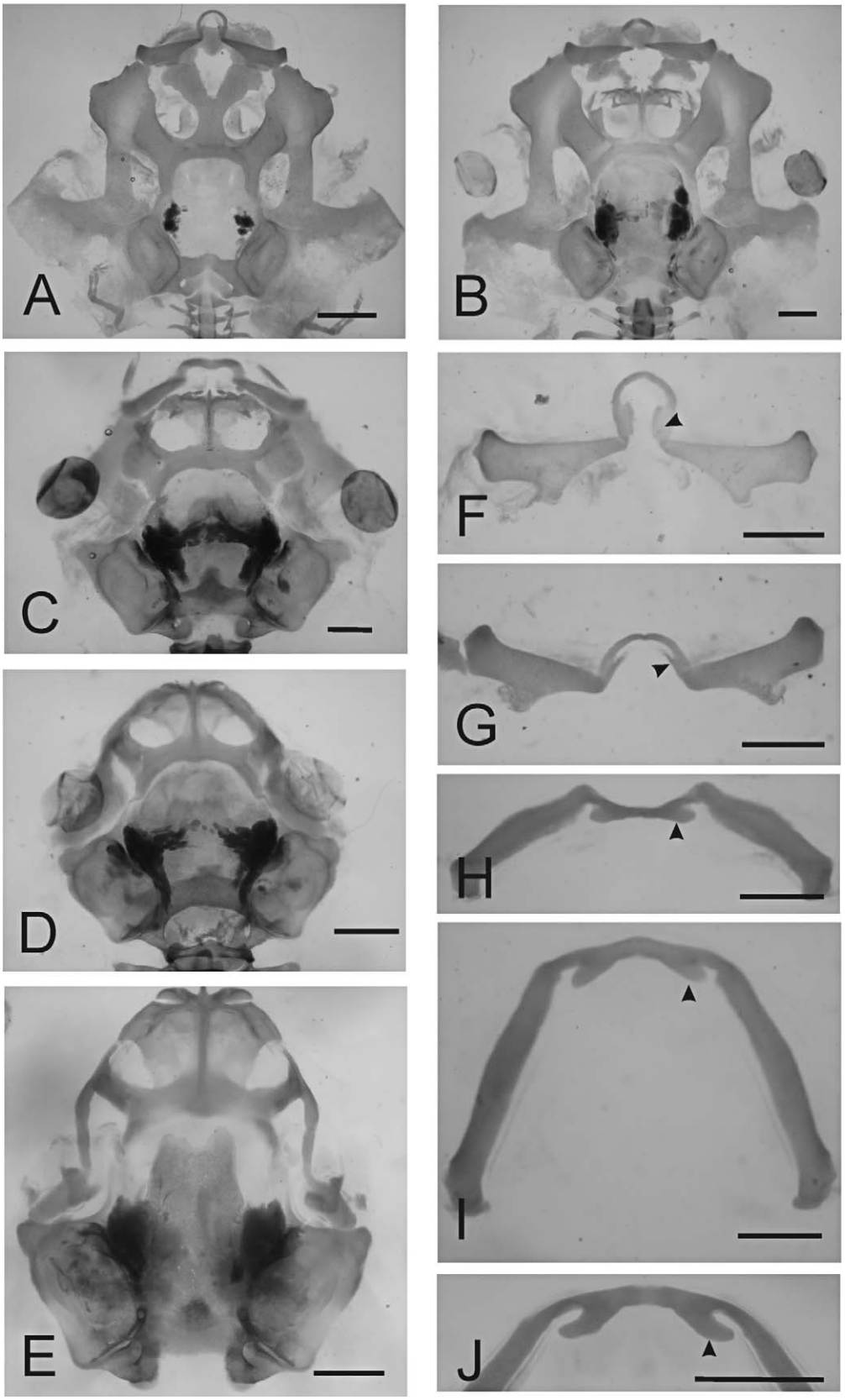

FIG. 6. Cartilage remodeling during advanced larval stages. (A–E) Dorsal views of the chondrocranium. Scale bar = 0.5 mm. (A) Stage 35, the chondrocranium similar to that described for stage 38. (B) Stage 41. Differentiation of nasal walls and nasal capsules cartilages is underway. Erosion of suprarostral and cornua trabeculae is advanced. (C) Stage 42. Vestiges of the suprarostral alae appear as free cartilages. The cartilaginous skeleton of the nasal capsule is formed. Posterior attachments of the palatoquadrate to the neurocranium are eroded and resorption of the subocularis arch is evident. (D) Stage 44. The palatoquadrate has changed abruptly. The processus pterygoideus is well differentiated and it is the new cartilaginous union of the upper jaw to the skull. The pars articularis of the palatoquadrate migrated backwards concomitant with the growth of the processus

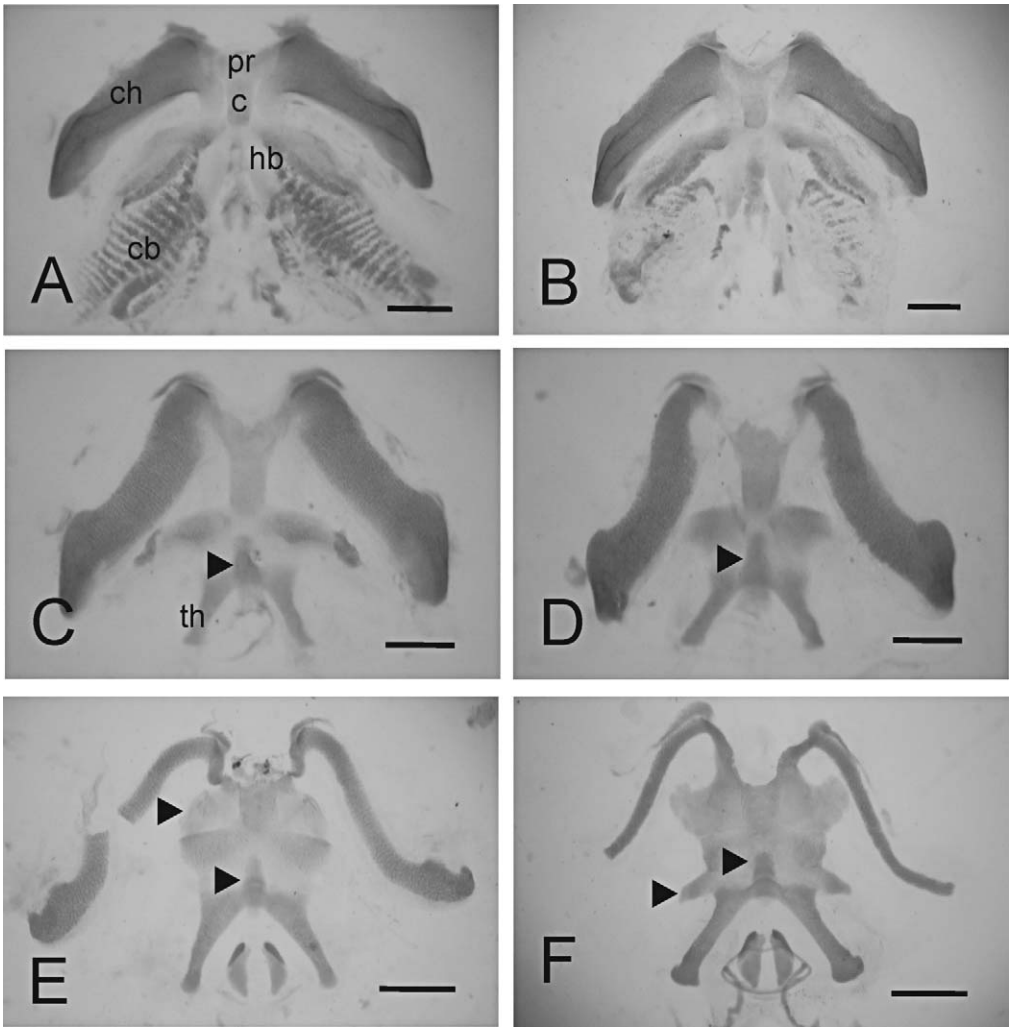

FIG. 7. Transformations of hyoid and branchial skeleton. Scale bar = 1 mm. (A) Stages 41. (B) Stage 42. Disappearance of ceratobranchials. (C) Stage 43. Differentiation of a cartilaginous condensation (Cartilage Z) between the hypobranchial plates. The adult posteromedial processes will grow from the hypobranchial plates. (D) Stage 44. The larval ceratohyals, pars reuniens, copula, and hypobranchial plates form a continuous single piece. (E) Stage 45. Arrow indicates additional new cartilage lateral to the copula developing into the anterolateral processes. The ceratohyals become slender. (F) At stage 46, new cartilage gives rise to the posterolateral processes and fuse to the hyoid plate. Cartilage Z is incorporated between the posteromedial processes and forms a protuberance for the attachment of the muscle hyoglossus. Abbreviations: c, copula; cb, ceratobranchial; ch, ceratohyal; hb, hypobranchial; pr, pars reuniens; and th, tirohya.

At stage 45 (Fig. 6E), the nares have a terminal position in dorsal view. The snout projects forward and beyond the lower jaw. The pars articularis of palatoquadrate is reduced and attaches by ligaments to the otic capsule; a poorly developed medial processus basalis is present. The cartilaginous lower jaw has distinct boundary between Meckel's cartilage and infrarostral, a well-developed mandibular symphysis, and the prominent Meckelian diverticula (Fig. 6I).

The transformation of the larval chondrocranium is complete at stage 46. The skull is short and the braincase is wider posteriorly than anteriorly. Cartilaginous elements roofing the cavum cranii did not develop. The occipital condyles flank the foramen magnum and are widely separated. The lower has a medial cartilaginous symphysis (Fig. 6J)

The larval hyobranchial skeleton is characterized by 1) slender, transverse ceratohyalia with well-defined anterior, medial, lateral, and posterior processes; 2) a broad pars reuniens; 3) an elongated copula with a long processus urobranchialis; 4) small, unfused hypobranchialia; and 5) four ceratobranchialia with numerous and elaborated rays. The ovoid branchial baskets extend from the level of the solum nasi to the level of Presacral Vertebra IV.

Metamorphic changes begin at stage 40 (Fig. 7A) with the rapid resorption of the ceratobranchialia in a posterior-to-

pterygoideus. (E) At stage 45, morphological changes in the palatoquadrate are completed; the cartilaginous configuration of the skull is that of the adult. (F–J) Changes in lower jaw. Scale bar = 1 mm. (F) Dorsal view of lower jaw at larval stage 33. The Meckelian diverticula of the infrarostral appear as laminar expansions, infrarostral and Meckel's cartilages are joined by a syndesmosis. (G) Stage 39. Infrarostral and Meckel's cartilages are fused. (H) Stage 42. Meckelian diverticula become massive and positioned medially. (I) Stage 45. The lengthening of Meckel's cartilages is noticeable. (J) Stage 46. The infrarostral is almost completely incorporated into the cartilaginous lower jaw. The mandibular symphysis is clear and the cartilaginous Meckelian diverticula are prominent.

anterior direction, and from Ceratobranchial IV to I. The hypobranchialia fuse medially and have a pair of posterior projections delimiting the laryngeal sinus.

During stage 41 (Fig. 7B), the anterior, lateral, and posterior processes of each ceratohyal have begun to erode. A medial chondrification—identified here as Cartilage Z—develops ventral to the hypobranchial plate and extends forward from the laryngeal sinus. The developing hyoglossus muscle attaches to the posterior margin of Cartilage Z.

At stage 43 (Fig. 7C), the hyobranchial skeleton still has identifiable larval ceratohyalia, pars reuniens, copula, and hypobranchialia; however, these elements form a single, contiguous, cartilaginous complex. Each robust ceratohyal still retains the rounded processus hyoquadratum. The pars reuniens and copula are approxiamtely twice their original lengths. The hypobranchial region has lateral projections with remains of the eroding Ceratobranchial I that will differentiate into the posterolateral processes. On the hypobranchial plate, the posterior processes have reshaped into well-differentiated posteromedial processes.

During stage 44 (Fig. 7D), the ceratohyalia become slender and have an oblique position; the hyoglossal sinus is now well defined.

At stage 45 (Fig. 7E), each ceratohyal still possess rounded tip representing the vestige of the larval processus hyoquadratum. The anterolateral process of the adult hyoid apparatus forms from new cartilages lateral to the copula. The posteromedial processes have well-differentiated distal epiphyses.

Stage 46 marks the end of the metamorphic changes in the hyobranchial apparatus (Fig. 7F). The processus hyoquadratum has disappeared and the ceratohyal is uniformly slender. New cartilages give rise to the posterolateral processes on the hyoid plate. Cartilage Z is incompletely incorporated into the edge of the hyoid plate between the posteromedial processes. At this stage, the cartilaginous hyoid apparatus acquires the adult configuration and appearance.

The posteromedial processes ossifies postmetamorphically. Cartilage Z is incorporated into the ventral edge of the hyoid, ossifies as a spurlike process between the ossifications of the posteromedial processes, and projects ventrally. In adults, a medial and anterior mineralization develops on the hyoid plate that corresponds to a mineralized larval copula.

Development of Postmetamorphic Traits.—Some anuran morphological features traits have little or no function in larvae, but they are necessary components of the adult body plan. Among those that we consider herein are the gonads, tongue, thyroid glands, limbs, bony skull, and plectral apparatus.

At stage 26, the gonads are undifferentiated and resemble whitish, elongated, cylindrical, and paired cords diverging caudally; the left cord is larger than the right (Fig. 5F). In stage 38, the undifferentiated organs are thin, laterally compressed cords. During metamorphosis, at stage 43, the gonads remain undifferentiated (Fig. 5G).

The tongue (Fig. 5H–K) is first evident in stage 36 as an anterior anlage on the buccal floor. The anlage grows, conserving its initial cordiform shape until stage 42, when the tongue lengthens posteriorly and develops a pointed end that becomes rounded in stage 44. At the end of metamorphosis, the tongue is ovoid and occupies the entire buccal floor. The paired hyoglossus muscles begin to differentiate in the tongue in stage 40; each muscle grows posteriorly and the number of muscle fibers increases. By stage 42, the tendon of the hyoglossal muscle fibers attaches to the developing Cartilage Z on the hyobranchial apparatus. The muscles lengthen and by stage 46 they are firmly attached to the protuberance formed by Cartilage Z.

Beginning at stage 36, the gland, follicle, and colloid volumes gradually increase and the epithelial cells become higher. There is no significant or abrupt variation of the thyroid glands during subsequent metamorphic stages (Figs. 5L–O, 8A–D).

Primary cartilages of limbs are differentiated by stage 34. The carpus is composed of seven cartilaginous elements (ulnare-intermedium, radiale, Distal Carpal 5+4+3, Distal Carpal 2, and Element Y). The tarsus comprises six distinct cartilages distal to the enlarged proximal tarsals (fibulare-tibiale) (Distal Tarsals 3, 2, and 1, the proximal prehallical element in the dorsal plane, and two primary cartilages that form Element Y in the ventral plane). Fusion of Distal Tarsals 3 and 2, as well as the formation of Element Y (by fusion of the two primary cartilages) occur at the end of stage 35.

The humerus is the first bone to ossify in the forelimb at stage 33, closely followed by the radius and ulna that are not fused yet. The ossification of the hind limb begins at stage 34, slightly after the ossification in the forelimb. Ossification of autopodia begins before all the cartilaginous phalanges have differentiated. Before the beginning of metamorphosis, at stage 40, all diaphyses of limbs have ossification centers. The ossification sequences of the hand and foot progress in proximal–distal and postaxial–preaxial directions. Ossification of the carpals, prepollex, distal tarsals, and prehallux occurs after metamorphosis.

At the end of stage 37, the endochondral ossification of the exoccipitals develops around the jugular foramen and extends toward the perilymphatic foramina.

By stage 38, the dermal parasphenoid has a broad cultriform process and short alae that cover the cranial floor and partially overlap the otic capsules. The endochondral ossification of the prootics begins on the inner wall of the otic capsule and expands anteriorly from the auditory foramina to surround the prootic and oculomotor foramina in the orbital cartilage.

In stage 39, each frontoparietal differentiates and grow medially; the frontoparietals grow rapidly and expand broadly behind the orbit.

At stage 40, the nasals appear over the developing cartilages of the nasal capsules. The septomaxillae, maxillae, and premaxillae are well differentiated by stage 41. The septomaxilla is a convex, laminar ossification attached to the developing oblique and alaris cartilages. Each premaxilla is a triangular bone with the ventral surface resting on the cornu trabecula. The maxilla ossifies anterior to the planum triangularis.

At stage 42 (Fig. 9A–C), the squamosal is a tiny, horizontal ossification attached to the base of the eroded processus muscularis of palatoquadrate. In the lower jaw, two ossifications develop anteriorly on Meckel's cartilages; the dentary differentiates along the labial surface and the angulosplenial on the lingual surface.

Subsequently, jaw and suspensorium bones (dentaries, angulosplenials, maxillae, and squamosals) and mandibular cartilages grow posteriorly. The ventral ramus of the squamosal gradually becomes vertical, along with the palatoquadrate and pars articularis; short rami (i.e., zygomatic and otic) develop and differentiate from the ventral ramus (Fig. 9D–L).

At stage 45, the quadratojugals and pterygoids are differentiated. The pterygoid, is attached to the posterior end of the processus pterygoideus of the palatoquadrate and remains small until the end of the metamorphosis, whereas the

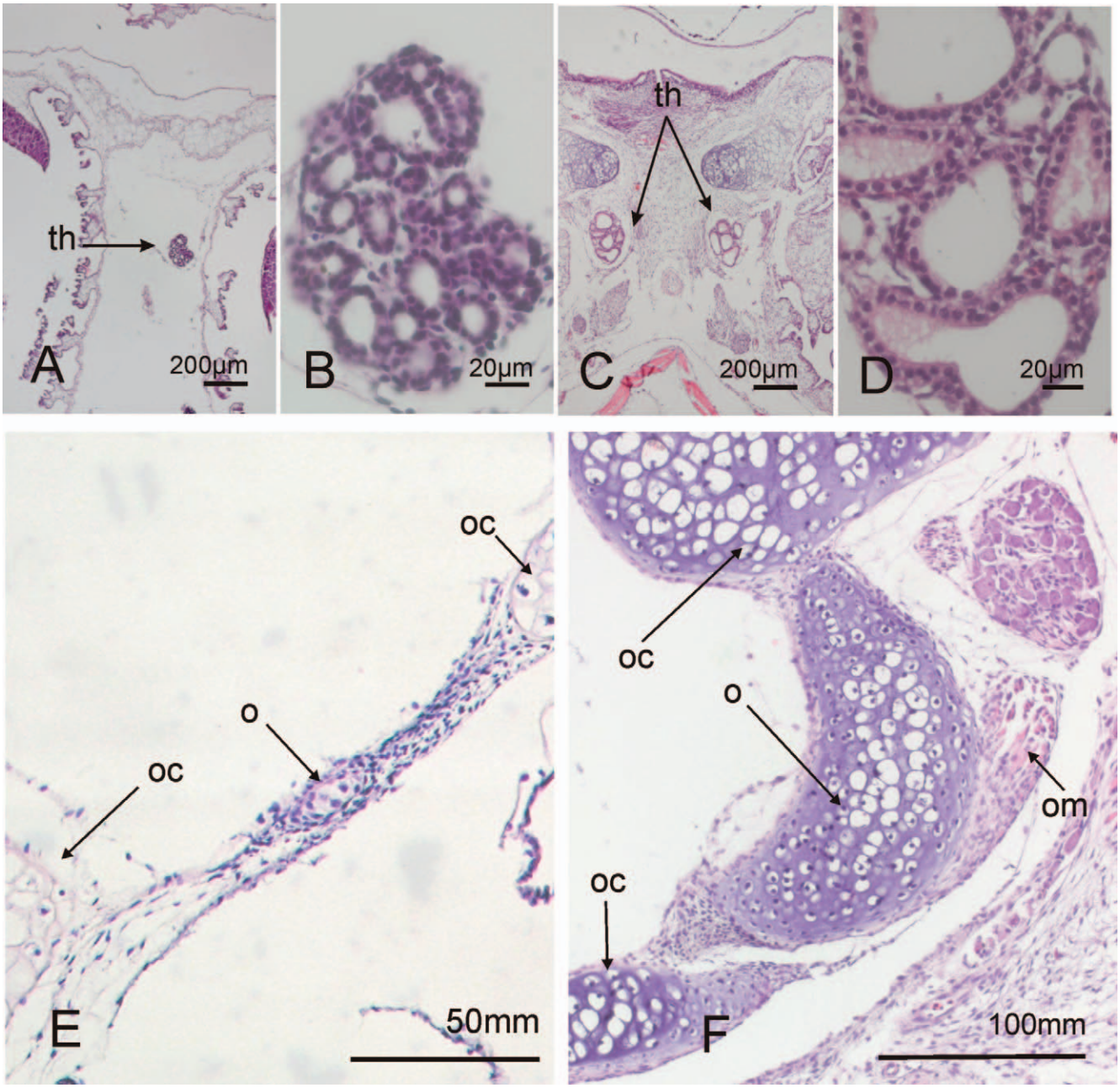

FIG. 8. (A–D) Histological changes in the thyroid glands. (A–B) Stage 35, the glands are organized into follicles, each containing a central lumen, and some lumina are beginning to accumulate colloid. The follicles are lined by a single layer of cuboidal epithelial cells. (C–D) Stage 43, the thyroids present enlarged follicles containing colloid and vacuoles within the colloid. (F–G) Transverse sections of at level of the otic capsule. (F) Stage 35, showing the incipient operculum in the fenestra ovalis. (G) Stage 43, the operculum is differentiated as well as the muscle opercularis. Abbreviations: o, operculum; oc, otic capsule; om, opercularis muscle; and th, thyroid gland.

quadratojugal grows anteriorly to articulate with the maxilla (Fig. 9M–O).

Ossification of cranial bones begins during larval development; however, the most extensive ossification of the skull takes place during postmetamorphic growth (Fig. 10A, B). Frontoparietals form a wide roof to the cavum cranii but they do not fuse medially. The large nasals completely cover the olfactory capsules and the alary cartilages and the processus prenasalis project forward over the anterior margins of the nasals. The superior and inferior prenasal cartilages are hidden by the premaxillae. The processus prenasalis, solum nasi, and septum nasi are mineralized. In ventral view, the ossification of the sphenethmoid extends to the premaxillary–maxillary articulation; neopalatines are absent (Fig. 10B). The sphenethmoid is not visible in dorsal view and forms an incomplete ring around the anterior end of the braincase; the two halves do not contact ventrally. The otic capsules are well ossified and the prootics are indistinguishably fused with the exoccipitals. The occipital condyles are widely separated. The ossification of the prootic extends anteriorly into the pila antotica; the prootic and oculomotor foramina are completely surrounded by this ossification. The mineralized crista parotica is wide, flat, and stout. Ossification of the braincase is extensive and contrasts with the reduced ossification of the jaws. Premaxillae and maxillae are edentulous. Each premaxilla has a rectangular pars palatine with a reduced processus palatinus. The pars alaris of

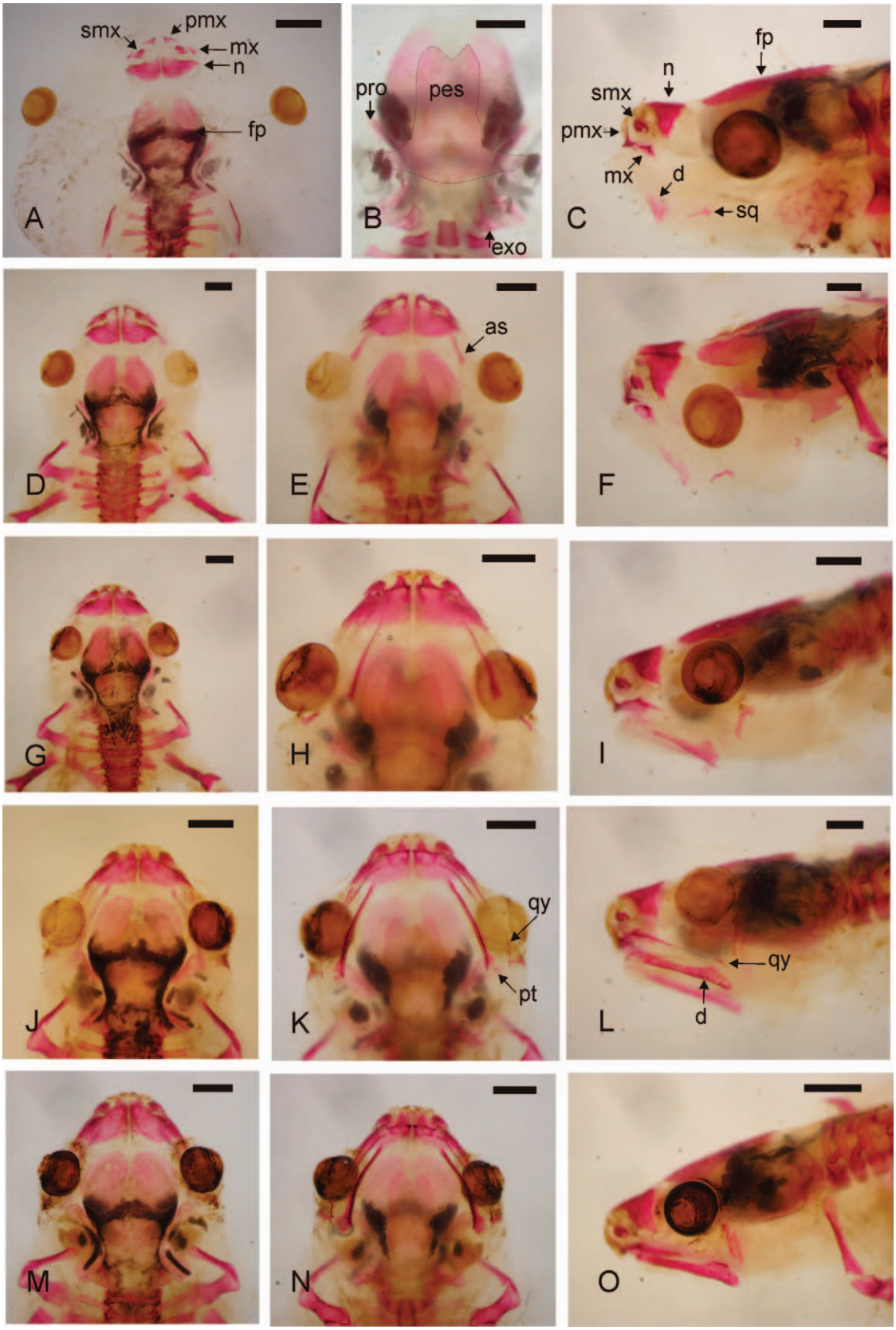

FIG. 9. Sequence of ossification. Scale bar = 1 mm. Left column is dorsal view, central column is ventral view, and right column is lateral view. (A–C) Stage 42. Ossification of nasals (n), frontoparietals (fp), septomaxillae (smx), exoccipitals (exo), and prootics (pro) are advanced, and differentiation of premaxillae (pmx), maxillae (mx), squamosals (sq), dentaries (d), and angulosplenials (as) progresses. (D–F) Stage 43. (G–H) Stage 44. The squamosal turns and has a vertical position. Short zygomatic and otic ramii are differentiated. (J–L) Stage 45. The quadratojugals and pterygoids have appeared. (M–O) Stage 46. The skull at the end of larval development is incompletely ossified. The pterygoid is a tiny ossification adjacent to the internal face of squamosal and attached to the posterior end of the cartilaginous pterygoid processus of the palatoquadrate.

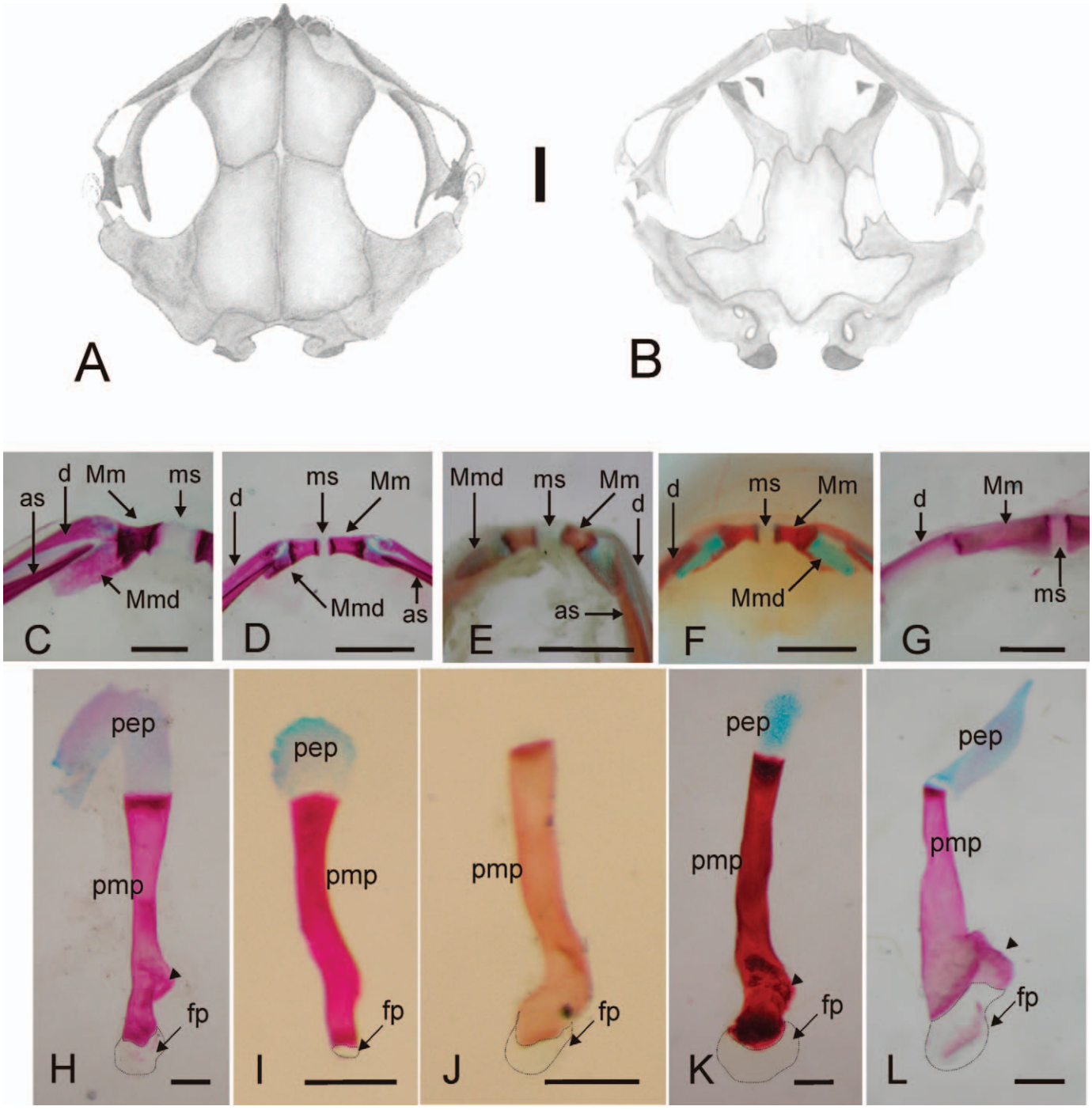

FIG. 10. (A–B) Dorsal and ventral views of the adult skull of *Dermatonotus muelleri*. Scale bar = 2 mm. (C–G) Adult morphology of the medial lower jaw elements in selected anurans. Abbreviations: as, angulosplenial; d, dentary; Mm, mentomeckelian; Mmd, Meckelian diverticulum; and ms, mandibular symphysis. Scale bar = 1 mm. (C) *Dermatonotus muelleri*. (D) *Elachistocleis bicolor*. (E) *Gastrophryne carolinensis*. (F) *Phrynomantis bifasciatus*. (G) *Scinax acuminatus*. (H–L) Adult morphology of the stapes in selected anurans depicting the non-expanded footplate of microhylids. Scale bar = 0.4 mm. (H) *D. muelleri*. (I) *E. bicolor*. (J) *G. carolinensis*. (K) *P. bifasciatus*. (L) *S. acuminatus*. Abbreviations: fp: footplate; pep, pars externa plectrum; and pmp, pars media plectrum.

the premaxilla is short and vertical; it is visible only in frontal view. The pars facialis of the maxilla is low, without a differentiated processus nasalis, and the pars palatina is reduced. The quadratojugal is tiny and touches, but does not overlap, the posterior tip of the maxilla. The ventral ramus of the squamosal is short and vertical, and the otic and zygomatic rami are poorly differentiated. The ossification of the squamosal does not contact the otic capsule. The anterior ramus of the pterygoid lingually invests the pterygoid process throughout the posterior half of the maxilla, whereas the medial ramus is short and does not reach the otic capsule. The posterior ramus of the pterygoid terminates at the cartilaginous pars articularis of the palatoquadrate. The cartilaginous attachments of the upper jaw to the skull do not stain with Alcian Blue. The vomers are small, thin, and triangular "scales" located along the anteromedial margins of the choanae. On the lower jaw (Fig.

10C), cartilaginous remains of Meckel's cartilages are visible between the dentaries and the angulosplenials. Each mentomeckelian is a cylindrical ossification lateral to the spheroid condensation of the mandibular symphysis. The mentomeckelian bone becomes continuous with the dentary through a mineralized bridge; lateral to the mandibular symphysis, each mentomeckelian projects ventrally investing the Meckelian diverticulum. This feature is similar to other microhylids (Fig. 10D–F) but differs from other anurans (Fig. 10G). Ossification of the sphenethmoid, vomers, and mentomeckelian are postmetamorphic events.

For the middle-ear apparatus, at stage 35, histological sections of the membrane covering the fenestra ovalis show connective tissue with few, parallel, elastic fibers and small fibroblasts surrounding the anlage of the operculum (Fig. 8E). The anlage is composed of a small oval group of round, basophilic cells with spherical nuclei; the cells are immersed in a matrix lacking fibers and lacunae. The organization of this connective membrane is looser toward the periphery. In whole-mounted specimens, the operculum gradually becomes Alcian Blue positive; it grows to fill the fenestra ovalis and is well defined at stage 40. At stage 43, the well-differentiated operculum consists of condensed hyaline cartilage surrounded by a thin layer of connective tissue (i.e., the remains of the original membrane). Histological sections show chondrocytes and large lacunae placed medially and a more uniform, extracellular matrix at the perichondral limits (Fig. 8F). The perichondrium of the operculum is continuous with the cartilaginous dorsal margin of the fenestra ovalis. The developing myoblasts of the opercularis muscle appear directly attached to the external, ventrolateral surface of the operculum.

The components of the stapes and the tympanic annulus develop during postmetamorphic stages (Fig. 10H). The stapes is slender and long, visible in dorsal and ventral views, and oriented obliquely towards the squamosal. The cartilaginous pars externa plectri is small. The tympanic annulus is sickle-shaped. The tympanic membrane is absent.

Discussion

The Microhylidae comprises 487 described species (Frost, 2011) that usually are medium- to small-sized species; however, there are several miniature and a few large taxa. Most species have free-swimming and feeding tadpoles, although nonfeeding tadpoles, direct development, or both have evolved independently in many lineages (Clarke, 1996; Glaw and Vences, 2007). Species with free-swimming and feeding tadpoles are characterized by "explosive" seasonal breeding in ephemeral ponds; some may breed multiple times during one season, and tadpoles of different ages are found simultaneously in the same pond. Most available descriptions report that microhylid larval development lasts from 20 to 60 days (Krügel and Richter, 1995), with larvae reaching a maximum total size of 40 mm and maximum SVLs at metamorphosis of no more than 16 mm (Cei, 1981; Donelly et al., 1990; Chou and Lin, 1997; Vera Candioti, 2006; Glaw and Vences, 2007; Lehr et al., 2007).

Dermatonotus muelleri inhabits the semiarid environments of the Chaco Region in South America; its reproduction occurs explosively three or four times during the wet season on warm days with heavy rainfall. Like other microhylids (e.g., *Elachistocleis bicolor*), *D. muelleri* deposits eggs as a film on the surface of the water (Lavilla et al., 1995) and larval development corresponds to the typical biphasic life style of microhylids of tropical and subtropical habitats, conforming overall with the life-history patterns described above.

The end of the larval period in *D. muelleri* is marked by the absence of the tail and the beginning of the terrestrial life style (Fig. 11). Froglets are small (14 mm), and significant postmetamorphic growth is needed to reach the adult size (40–50 mm). Females are larger than males and gonad differentiation occurs during postmetamorphic stages; rates of body growth could be related to differentiation and maturation of ovaries and testes. Under natural conditions, the development (i.e., from fertilization to metamorphosis) of *D. muelleri* lasts between 22 and 26 days. The period between stages 41 and 46 corresponds to metamorphic climax and at a maximum, lasts 3 days. By stage 37, tadpoles have attained their metamorphic snout–vent size; this seems to distinguish larvae of *D. muelleri* from other Type-IV tadpoles in which the snout–vent size increases until the forelimbs emerge (Hall et al., 1997; Quinzio et al., 2006; Fabrezi, 2011). Larval somatic growth and metamorphic development seem to parallel each other in most anurans; thus, one might expect that any negative external factor (e.g., diet, temperature, competence, and predation) might affect the rate of development and modify somatic growth or vice versa (Wilbur and Collins, 1973). However, the early acquisition of maximum larval somatic growth (i.e., metamorphic size) in *D. muelleri* suggests that size would not be affected by later changes in larval developmental rate.

The loss of larval features during development in *D. muelleri* occurs between stages 41 and 46 (Fig. 11); structures are lost in the following sequence: 1) vent tube, 2) larval mouth, 3) lateral line system, 4) spiracle, and 5) tail. At the same time (i.e., stages 41–46), internal larval tissues are undergoing transformation. The synchrony of the onset and offset of transformations in digestive tract, jaws, and the hyoglossal apparatus is associated with the development of the adult feeding mechanism. The onset of ossification of the limbs and skull at stage 34 indicates these events are partially independent of other anatomical larval components (Fig. 11).

Tadpoles of *D. muelleri* have nine pairs of symmetrical lines of neuromasts. The distribution of these lines resembles the generalized pattern described for anurans except for the unusual lengths of ventral and angular lines that may be related to the medial position of the spiracle. The organization of the neuromasts within each lateral line, in irregular groups of five to seven organs, coincides with descriptions for other microhylids (Lannoo, 1987). Studies of the temporal and spatial sequences of the disappearance of the lateral line system reveal that the process starts simultaneously in receptor organs, ganglion cells, and central nuclei at metamorphic climax. The beginning of this process is correlated with high levels of circulating thyroid hormone and the expression of thyroid hormone receptors in the parts of the lateral line system mentioned (Wahnschaffe et al., 1987; Schlosser, 2002). These findings suggest that thyroid hormone triggers the disappearance of the lateral line system (Schlosser, 2002). In *D. muelleri*, all lateral lines begin to disappear almost simultaneously before the forelimbs emerge. The lateral-line system is lost while caudal fins and tail musculature are still well differentiated. This is in striking contrast to descriptions of other anurans (e.g., *Rana temporaria*, *Hyperolius mitchelli*, Wahnschaffe et al., 1987; *Pseudis paradoxa*, Fabrezi et al., 2009; ceratophryids, Quinzio, unpubl. data).

Limb development in *D. muelleri* has a spatial and temporal pattern of differentiation of primary cartilages and ossification

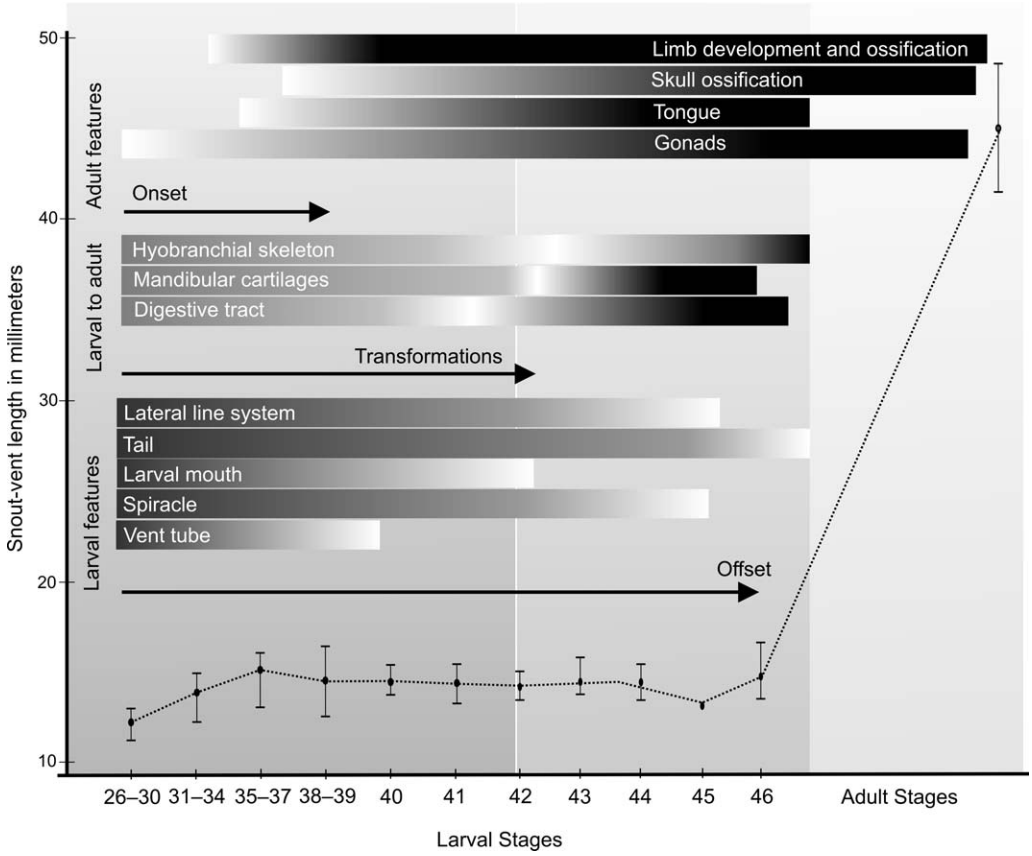

FIG. 11. Ontogenetic pattern of development and growth in *Dermatonotus muelleri*. Larval growth has an early offset quite simultaneously with the onset of limb ossifications. Some metamorphic transformations represent predisplacement with respect to forelimb emergence (i.e., the onset of changes in larval gut) or with respect to tail disappearance (the offset of transformations of jaw cartilages).

resembling that of other anurans (de Sá, 1988; de Sá and Trueb, 1991; Fabrezi and Alberch, 1996; Fabrezi and Goldberg, 2009). This suggests that developmental events related to adult anatomical structures are not closely linked to the development of species-specific unique larval structures. The endochondral ossifications of the diaphyses and some skull bones (e.g., exoccipitals and prootics) are the earliest to appear and continue development in postmetamorphic stages (Fig. 11). Dermal skull bones (e.g., those forming the floor and roof of the braincase and snout) are well differentiated at stage 41 (Fig. 11). However, dermal bones associated with the development of the jaw apparatus seem to be linked to changes in larval jaw cartilage. This pattern of ossification is in agreement with available reports on the ossification of most anurans (Trueb, 1985; de Sá and Trueb, 1991; among others).

Patterns of larval development and gonadal differentiation also are dissociated developmental events (Lopez, 1989; Ogielska and Kotusz, 2004). Differentiation of the gonads occurs before metamorphosis in species with long larval periods (e.g., *Pseudis* spp., Downie et al., 2009; Fabrezi et al., 2010) and after metamorphosis in species with short larval periods (e.g., *Scaphiopus couchii*, Buchholz and Hayes, 2005). *Dermatonotus muelleri* and other anurans with ecological similar breeding sites (e.g., *Scinax acuminatus*, *S. nasicus*, Fabrezi et al., 2010) have a moderately short larval period and delayed gonadal differentiation (Fig. 11).

Transformation of the digestive tract of *D. muelleri* begins before forelimb emergence at stage 41 with changes occurring in an anterior–posterior direction. The onset of other developmental changes related to adult feeding—but involving different cellular types, such as those of the skeleton, muscles, and nerves that will form the hyoglossal apparatus—occurs before stage 41 (Fig. 11).

Changes in the cartilaginous cranial skeleton and visceral arches in *D. muelleri* include the following coordinated events: 1) differentiation and development of the olfactory capsules concomitant to the resorption of the trabecular horns and suprarostral; 2) resorption of ceratobranchials and remodelling of ceratohyalia, pars reuniens, copula, and hypobranchialia to form the hyoid skeleton; and 3) lower jaw elongation concomitant to the resorption of the palatoquadrate-neurocranium attachments and differentiation of new cartilaginous connections. These changes are synchronous with each other and precede the development and/or changes that will occur in the musculature and bony skeleton. For example, olfactory cartilages appear before bones of the snout (nasals, vomers, and premaxillae). Changes in the hyobranchial skeleton advance accompany tongue development and differentiation of associated hyoglossus and genioglossus muscles, and changes in the palatoquadrate and lower jaw begin just before transformations of the mandibular and hyoid muscles and the differentiation of the mandibular bones (maxillae, squamosals, pterygoids, and quadratojugals). Endochondral ossification of the braincase occurs without major remodelling of cartilages before metamorphic events. The dermal cranial ossification of *Hamptophryne boliviana* is delayed and occurs after metamorphosis (de Sá and Trueb, 1991); however, cartilage remodelling is similar to *D. muelleri*.

During the development of *Dermatonotus muelleri*, as well as that of *H. boliviana* (de Sá and Trueb, 1991), transformations of larval jaws reflect a low developmental rate in which the offset of the palatoquadrate/infrarostal-Meckel's cartilages lengthening at the end of metamorphosis exhibits the condition that most anurans reach at the middle of metamorphosis (stage 44) (Fabrezi, 2011). Paedomorphic features of cartilaginous jaws impact the development of the associated bones that are either reduced (e.g. vomers, quadratojugals) or absent (e.g. neopalatines).

Microhylid skulls are characterized by the anterior location of the lower jaw articulation (Zweifel, 1985; de Sá and Trueb, 1991; Lehr and Trueb, 2007). Ossification of the squamosal and pterygoid provides weak reinforcement to the cartilaginous suspensorium. The ventral ramus of the squamosal is nearly vertical and short, the zygomatic ramus is usually small but variable in its development, and the otic ramus is reduced or absent; furthermore, the squamosal does not contact the otic capsule. The pterygoid also has short posterior and medial rami. In addition, quadratojugals, vomers, and palatines may be absent; if present, they are small or less differentiated. The position of the jaw articulation defines a small mouth gape that is characteristic of several adult microhylids.

Trueb and Alberch (1985) described the sequence of appearance of anuran skull bones; furthermore they proposed that paedomorphic cranial patterns could be related to the overall small size of some species given that loss of skull bones (e.g., neopalatines, vomers, quadratojugals) is infrequent in large-sized species. Yeh (2002) explored anuran intraordinal variation in adult sizes, skull shapes, and skull bones and described some patterns that could be predictive for clades that exhibit size reduction. Despite limited knowledge of the developmental variation within Microhylidae, skull development, skull shape, and skull bone loss in *Dermatonotus muelleri* suggests that these features are a consequence of larval morphology and gradual metamorphosis of the cartilaginous upper and lower jaws (Wassersug and Hoff, 1982).

In *Dermatonotus muelleri* the anterior medial segment of the larval lower jaw consists of a single piece. Vera Candioti (2006, 2007) described it as fused infrarostrals and de Villiers (1930) demonstrated the absence of a discernible symphysis through histological sections of the jaw of *Phrynomantis bifasciatus*. Two infrarostrals joined by a copula mandibularis were reported in *H. boliviana* (de Sá and Trueb, 1991). Whether New World microhylids have a single or paired infrarostrals needs to be demonstrated with supporting histological evidence from early developmental stages. However, it is worthwhile to highlight that during the metamorphosis of *D. muelleri*, the contribution of the infrarostrals to the formation of the cartilaginous skeleton of the adult lower jaw is limited to their most anterior segments that include the Meckelian diverticula (Fig. 6F–J). This fact is different from other anurans in which the metamorphic lengthening of the infrarostrals contributes to form up to the 30% of the adult cartilaginous jaw (Fabrezi, 2011:fig. 6). At least in the microhylid *D. muelleri*, the anterior placement of the jaw articulation is both the result of the larval morphology of the infrarostal and the early offset of the metamorphosis of the jaw.

Another feature related with the skull configuration of microhylid frogs is the reduction of the tympanic system. *Dermatonotus* and other microhylids lack a tympanic membrane but have a well-developed plectral apparatus as well as the tympanic annulus that differentiates during postmetamorphic growth. The pars interna and media plectri form a slender, long, and well-ossified bar reaching the squamosal (Fig. 10C–F vs. Fig. 9G). The pars externa plectri is a small and oval cartilage surrounded by a small and incomplete tympanic annulus. Absence of the tympanic membrane and reduction in size of the tympanic annulus and pars externa plectri in *Dermatonotus* and other microhylids could be related with the paedomorphic characteristics of the palatoquadrate (Smirnov and Vorobyeva, 1988). Interspecific comparisons of the plectral apparatus in microhylids reveal they could be characterized by the reduction of the footplate (Fig. 10C–F).

In summary, the tadpole of *D. muelleri* corresponds to the Orton's morphotype II (Microhyloidea), and it is characterized by an accumulation of several apomorphic features, some of which are unique among anuran larvae (Haas, 2003). Larval development in *D. muelleri* (Fig. 11) reveals an interesting pattern in which remodeling of larval into adult jaws during metamorphosis has an early offset with consequences in the differentiation and development of the bony skull. The morphological changes observed in *D. muelleri* begin at larval stage 35; moreover, they have been related to the thyroid glands' function in anurans with free-swimming larvae and direct development (Etkin, 1936; Jennings and Hanken, 1998; Callery and Elinson, 2000). Standard developmental tables based on Type-IV larvae traditionally define the beginning of metamorphic climax by forelimb emergence (that also involves spiracle disappearance), loss of larval mouthparts, and onset of transformations in the gut and visceral arches (mandibular and hyobranchial skeleton) (Etkin, 1936; Gosner, 1960). Within this context, the developmental sequences in *D. muelleri*, as well as that of other anurans, such as *Pseudis* spp. (Fabrezi et al., 2009, 2010; Fabrezi, 2011), ceratophryines (Fabrezi and Quinzio, 2008; Fabrezi, 2011), and *Sphaenorhynchus bromelicola* (Bokermann, 1974), suggest that the onset of metamorphic changes varies and is not fixed as might be inferred from standard anuran developmental tables. However, the end of larval development is marked by the complete loss of the tail, an ontogenetic event in which changes in larval developmental modules undergo integration with those of the adult stages to converge in the unique adult body plan that seems to be independent with larval growth.

A more comprehensive taxonomic revision of larval morphology, larval development, and their variation among microhylids could provide help to understand the morphological evolution in the group.

Acknowledgments.—We thank an anonymous reviewer for comments on reformatting the manuscript to conform to journal style. We are grateful to G. Gonzo and F. Hongn for assistance in the field; to Secretaría de Medio Ambiente y Desarrollo Sustentable, Gobierno de la Provincia de Salta for permission to collect the specimens for this study; and to S. Blanco and P. Villagrán, who provided technical assistance at the Laboratorio de Microscopía Electrónica de Barrido, Universidad Nacional de Salta. This research was supported by CONICET, PIP 239 to MF.

Literature Cited

Altig, R. I., and G. F. Johnston. 1989. Guilds of anuran larvae: relationships among developmental modes, morphologies, and habitats. Herpetological Monographs 3:81–109.

Bokermann, W. C. A. 1974. Observações sobre desenvolvimento precoce em *Sphaenorhynchus bromelicola* Bok. 1966 (Anura, Hylidae). Revista Brasileira de Biologia 34:35–41.

Bozzola, J. J., and L. D. Russell. 1999. Electron microscopy. *In* Principles and Techniques for Biologists. Jones and Bartlett Publishers, Sudbury, MA.

Buchholz, D. R., and T. B. Hayes. 2005. Variation in thyroid hormone action and tissue content underlies species differences in the timing of metamorphosis in desert frogs. Evolution and Development 7: 458–467.

Callery, E. M., and R. P. Elinson. 2000. Thyroid hormone-dependent metamorphosis in a direct developing frog. Proceedings of the National Academy of Sciences of the United States of America 97: 2615–2620.

Cei, J. M. 1981. Amphibians of Argentina. Monitore Zoologico Italiano, N. S. Monographia 2:1–609.

Chou, W.-H., and J. Lin. 1997. Tadpoles of Taiwan. National Museum of Natural Sciences in Taiwan, Special Publication 7:1–98.

Clarke, B. T. 1996. Small size in amphibians: its ecological and evolutionary implications. Symposia of the Zoological Society of London 69:201–224.

de Sá, R. O. 1988. Chondrocranium and ossification sequence of *Hyla lanciformis*. Journal of Morphology 195:345–355.

de Sá, R. O., and L. Trueb. 1991. Osteology, skeletal development, and chondrocranial structure of *Hamptophryne boliviana* (Anura: Microhylidae). Journal of Morphology 209:311–330.

De Villiers, C. G. S. 1930. On the cranial characters of the South African brevicipitid, *Phrynomerus bifasciatus*. Quarterly Journal of Microscopical Science 73:667–705.

Donelly, M. A., R. O. de Sá, and C. Guyer. 1990. Description of the tadpole of *Gastrophryne pictiventris* and *Nelsonophryne atterrima* (Anura: Microhylidae), with a review of morphological variation in free-swimming microhylid larvae. American Museum Novitates 2976:1–19.

Downie, J. R., R. Bryce, and J. Smith. 2004. Metamorphic duration: an under-studied variable in frog life histories. Biological Journal of the Linnean Society 83:261–272.

Downie, J. R., K. Sams, and P. T. Walsh. 2009. The paradoxical frog *Pseudis paradoxa:* larval anatomical characteristics, including gonadal maturation. Herpetological Journal 19:1–10.

Duellman, W., and L. Trueb. 1986. Biology of Amphibians. The John Hopkins University Press, Baltimore, MD. 670 p.

Etkin, W. 1936. The phenomena of anuran metamorphosis. III. The development of the thyroid gland. Journal of Morphology 59:69–89.

Fabrezi, M. 2011. Heterochrony in growth and development in anurans from the Chaco of South America. Evolutionary Biology 38:390–411.

Fabrezi, M., and P. Alberch. 1996. The carpal elements of anurans. Herpetologica 52:188–204.

Fabrezi, M., and J. Goldberg. 2009. Heterochrony during skeletal development of *Pseudis platensis* (Anura, Hylidae) and the early offset of skeleton development and growth. Journal of Morphology 270:205–220.

Fabrezi, M., and S. I. Quinzio. 2008. Morphological evolution in Ceratophyinae frogs (Anura, Neobatrachia): the effects of heterochronic changes during larval development and metamorphosis. Zoological Journal of the Linnean Society 154:752–780.

Fabrezi, M., S. I. Quinzio, and J. Goldberg. 2009. The giant tadpole and the delayed metamorphosis of *Pseudis platensis* Gallardo, 1961 12 (Anura, Hylidae). Journal of Herpetology 43:228–243.

Fabrezi, M., S. I. Quinzio, and J. Goldberg. 2010. The ontogeny of *Pseudis platensis* (Anura, Hylidae): heterochrony and the effects of larval development in the postmetamorphic life. Journal of Morphology 271:496–510.

Ford, L., and D. C. Cannatella. 1993. The major clades of frogs. Herpetological Monographs 7:94–117.

Frost, D. R. 2011. Amphibian species of the world: an online reference. Version 5.4 [Internet]. Available from: http://research.amnh.org/vz/herpetology/amphibia/. American Museum of Natural History, New York.

Frost, D. R., T. Grant, J. Faivovich, R. H. Bain, A. Haas, C. T. B. Haddad, R. O. de Sá, A. Channing, M. Wilkinson, S. C. Donnellan, et al. 2006. The amphibian tree of life. Bulletin of American Museum of Natural History 297:1–370.

Glaw, F., and M. Vences. 2007. A Field Guide Amphibians and Reptiles of Madagascar. 3rd ed. Vences and Glaw Verlag, Köln, Germany.

Goldberg, J., and M. Fabrezi. 2008. Development and variation of the anuran webbed feet (Amphibia, Anura). Zoological Journal of the Linnean Society 152:39–58.

Gosner, K. L. 1960. A simplified table for staging anuran embryos and larvae with notes on identification. Herpetologica 16:183–190.

Haas, A. 2003. Phylogeny of frogs as inferred from primarily larval characters (Amphibia: Anura). Cladistics 19:23–89.

Hall, J. A., J. H. Larsen, and R. E. Fitzner. 1997. Postembryonic ontogeny of the Spadefoot Toad, *Scaphiopus intermontanus* (Anura: Pelobatidae): external morphology. Herpetological Monographs 11: 124–178.

——. 2002. Morphology of the Premetamorphic larva of the Spadefoot Toad, *Scaphiopus intermontanus* (Anura: Pelobatidae), with an emphasis on the lateral line system and mouthparts. Journal of Morphology 252:114–130.

Hall, J. A., and J. H. Larsen. 1998. Postembryonic ontogeny of the spadefoot toad, *Scaphiopus intermontanus* (Anura: Pelobatidae): skeletal morphology. Journal of Morphology 238:179–244.

Jennings, D. H., and J. Hanken. 1998. Mechanistic basis of life history evolution in anuran amphibians: thyroid gland development in the direct-developing frog, *Eleutherodactylus coqui*. General and Comparative Endocrinology 111:225–232.

Krügel, P., and S. Richter. 1995. *Syncope antenori*—a bromeliad breeding frog with free-swimming, non-feeding tadpoles (Anura, Microhylidae). Copeia 1995:955–963.

Lannoo, M. J. 1987. Neuromast topography in anuran amphibians. Journal of Morphology 191:115–129.

Larson, P. M., and R. O. de Sá. 1998. Chondrocranial morphology of *Leptodactylus* larvae (Leptodactylidae: Leptodactylinae): its utility in phylogenetic reconstruction. Journal of Morphology 238:287–305.

Lavilla, E. O. 1992. The tadpole of *Dermatonotus muelleri* (Anura: Microhylidae). Bolletino Museum Regionale de Science Naturale Torino 10:63–71.

Lavilla, E. O., F. B. Cruz, and G. Scrocchi. 1995. Amphibiens et reptiles de la Station Biologique "los Colorados" dans la province de Salta, Argentina. Revue Françáise d'aquariologie 1–2:51–58.

Lehr, E., and L. Trueb. 2007. Diversity among New World microhylid frogs (Anura: Microhylidae): morphological and osteological comparisons between *Nelsonophryne* (Günther 1901) and a new genus from Peru. Zoological Journal of the Linnean Society 149:583–609.

Lehr, E., L. Trueb, P. J. Venegas, and E. Arbelaez. 2007. Descriptions of the tadpoles of two Neotropical microhylid frogs, *Melanophryne carpish* and *Nelsonophryne aequatorialis* (Anura: Microhylidae). Journal of Herpetology 41:581–589.

Lopez, K. 1989. Sex differentiation and early gonadal development in *Bombina orientalis* (Anura: Discoglossidae). Journal of Morphology 199:299–311.

Martoja, R., and M. Martoja-Pierson. 1970. Técnicas de Histología Animal. Toray-Masson, S.A., Barcelona.

Nieuwkoop, P. D., and J. Faber. 1956. Normal Table of *Xenopus laevis* (Daudin). North Holland Publ. Co., Amsterdam.

Ogielska, M., and A. Kotusz. 2004. Pattern of ovary differentiation with reference to somatic development in anuran amphibians. Journal of Morphology 259:41–54.

Orton, G. I. 1953. The systematics of vertebrate larvae. Systematic Zoology 2:63–75.

Orton, G. I. 1957. The bearing of larval evolution on some problems in frog classification. Systematic Zoology 6:79–86.

Quinzio, S. I., M. Fabrezi, and J. Faivovich. 2006. Redescription of the tadpole of *Chacophrys pierottii* (Vellard, 1948) (Anura: Ceratophryidae). South American Journal of Herpetology 1:202–209.

Roelants, K., A. Haas, and F. Bossuyt. 2011. Anuran radiations and the evolution of tadpole morphospace. Proceedings of the National Academy of Sciences of the United States of America 108:8731–8736.

Schlosser, G. 2002. Development and evolution of lateral line placodes in amphibians. I. Development. Zoology 105:119–146.

Smirnov, S. V., and E. I. Vorobyeva. 1988. Morphological grounds for diversification and evolutionary change in the amphibian sound-conducting apparatus. Anatomischer Anzeinger 166:317–322.

Sokol, O. 1975. The phylogeny of anuran larvae: a new look. Copeia 1975:1–23.

Trueb, L. 1985. A summary of osteocranial development in anurans with notes on the sequence of cranial ossification in *Rhinophrynus dorsalis* (Anura: Pipoidea: Rhinophrynidae). South African Journal of Sciences 81:181–185.

Trueb, L., and P. Alberch. 1985. Miniaturization and the anuran skull: a case study of heterochrony. *In* H.-R. Duncker, and G. Fleisher (eds.), Vertebrate Morphology, pp. 113–121. Gustav Fischer Verlag, New York.

Vera Candioti, M. F. 2006. Morfología larval de *Chiasmocleis panamensis*, con comentarios sobre la variabilidad morfológica interna en renacuajos de Microhylidae (Anura). Alytes 24:91–108.

Vera Candioti, M. F. 2007. Anatomy of anuran tadpoles from lentic water bodies: systematic relevance and correlation with feeding habits. Zootaxa 1600:1–175.

Wahnschaffe, U., U. Bartsch, and B. Fritzsch. 1987. Metamorphic changes within the lateral-line system of Anura. Anatomy and Embryology 175:431–442.

Wassersug, R. J. 1976. A procedure for differential staining of cartilage and bone in whole formalin fixed vertebrates. Stain Technology 51: 131–134.

Wassersug, R. J., and K. Hoff. 1982. Developmental changes in the orientation of the anuran jaw suspension: a preliminary exploration into the evolution of anuran metamorphosis. Evolutionary Biology 15:223–246.

Wilbur, H. M., and J. P. Collins. 1973. Ecological aspects of amphibian metamorphosis. Science 182:1305–1314.

Yeh, J. 2002. The effect of miniaturized body size on skeletal morphology in frogs. Evolution 56:2628–2641.

Zweifel, R. G. 1985. Australian frogs of the family Microhylidae. Bulletin American Museum of Natural History 182:265–388.

Accepted: 17 October 2011.